Studies on the thermostabilization of reverse transcriptases from Moloney murine leukemia virus and avian myeloblastosis virus

Atsushi Konishi

2015

Contents

Abbreviations

AMV	avian myeloblastosis virus
CD	circular dichroism
cDNA	complementary DNA
dNTP	deoxynucleotide
DTT	dithiothreitol
E. coli	*Escherichia coli*
HIV	human immunodeficiency virus
IPTG	isopropyl 1-thio-β-D-galactoside
k_{cat}	molecular activity
K_d	dissociation constant
K_m	Michaelis constant
k_{obs}	first-order rate constant for thermal inactivation
MMLV	Moloney murine leukemia virus
PAGE	polyacrylamide gel electrophoresis
PCR	polymerase chain reacrtion
PMSF	phenylmethylsulfonyl fluoride
RNase	ribonuclease
RT	reverse transcriptase
T/P	template-primer
UV	ultraviolet
WT	wild-type enzyme
XMRV	xenotropic murine leukemia virus-related virus

Introduction

Retroviral reverse transcriptase (RT) [EC 2.7.7.49] possesses RNA- and DNA-dependent DNA polymerase as well as RNase H activities. Due to their high catalytic activity and fidelity (*1*), RTs from Moloney murine leukemia virus (MMLV) and avian myeloblastosis virus (AMV) are the most extensively used in conventional cDNA synthesis (*2*). They are also used in RNA-specific amplification, which is an isothermal reaction (41-43ºC) that specifically amplifies a target RNA sequence, with RNA polymerase (*3*, *4*). The MMLV RT is a 75-kDa monomer, whereas AMV RT is a heterodimer consisting of a 63-kDa α subunit and a 95-kDa β subunit. Structurally, MMLV RT is comprised of the fingers, palm, thumb, connection, and RNase H domains (*5*-*8*). This nomenclature, which was originally used in human immunodeficiency virus type 1 (HIV-1) RT (*9*), is based on the resemblance to a right hand. The α subunit of AMV RT is also comprised of these five domains, while the β subunit consists of these five domains as well as the C-terminal integrase domain (*10*). The active site of the DNA polymerase activity is located in the palm subdomain while residues in the fingers and thumb subdomains participate in nucleotide and primer binding. The active site of the RNase H activity resides in the RNase H domain.

Thermal stability of DNA polymerases is important for their wide-range practical use. For cDNA synthesis and RNA-specific amplification procedures, an elevated reaction temperature is highly desirable because it reduces RNA secondary structure and nonspecific binding of the primer. Thermostable DNA-dependent DNA polymerases that are currently used in the polymerase chain reaction (PCR), such as the one isolated

from *Thermus aquaticus* (*Taq*) (*11*), retain activity even after the incubation at >90ºC. However, unlike DNA polymerases, RT activity is not thermally stable. For example, the initial reverse transcriptase activities of MMLV and AMV RTs are reduced by 50% at 44 and 47ºC, respectively, during a 10-min incubation (*12*). Thermal stability of RT has been markedly improved by eliminating its RNase H activity (*13, 14*), resulting in an increase in reaction temperature from 37ºC to higher than 42ºC (*14*). However, RNase H-minus RT cannot be used in an RNA-specific amplification reaction because this procedure requires both DNA polymerase and RNase H activities. Therefore, the RNA-specific amplification reaction must still be performed at low temperatures around 41 to 43ºC (*15, 16*). Considering that RNA is stable up to 65ºC, further stabilization of RT would be desirable for cDNA synthesis. Improvement in the thermal stabilities of MMLV RT and AMV RT is therefore still an important goal.

The aim of this study is to generate thermally stabilized variants of MMLV and AMV RTs by site-directed mutagenesis and to explore the mechanism of stabilization of RTs. In Chapter 1, highly stable MMLV RT variants were generated by introducing basic residues in the nucleic acid binding cleft and in a surface hydrophobic residue of the RT. In Chapter 2, a new method for the production of AMV RT α subunit by using insect cells was established, and a stable AMV RT α subunit variant was generated by the mutations. In Chapter 3, the binding affinities and RNase H activities of the stable MMLV RT variants were examined to explore the thermostabilization mechanism of RTs. It is expected that this study will lead to expanded usage of MMLV and AMV RTs in cDNA synthesis and give important findings that would be valuable in further stabilizing of RTs.

Chapter 1

Thermostabilization of Moloney murine leukemia virus reverse transcriptase by site-directed mutagenesis

Introduction

As described in General Introduction, the thermostability of MMLV RT is low: the initial reverse transcriptase activities of MMLV RT in the absence and presence of T/P are reduced by 50% at 44 and 47ºC, respectively, during a 10-min incubation (*12*). Considering that RNA is stable up to 65ºC, generation of thermostable MMLV RT is an important subject. In the case of MMLV RT, recombinant enzymes expressed in *Eshcerichia coli* have been used in cDNA synthesis and structural analysis. Crystal structure of the fingers, palm, thumb, and connection domains (Thr24-Pro474) (*6*) and that of the RNase H domain (His503-Ser668) (*7*) have been independently determined, while that of the full length molecule has not been determined yet. In the structural analysis of the Thr24-Pro474, the variant enzyme L435K, but not the wild-type enzyme, was used because its solubility is higher than that of WT (*17*).

T/P has phosphate groups, which are negatively charged in the neutrality conditions. Therefore, we have hypothesized that the introduction of positively-charged residues into MMLV RT will improve its ability to bind T/P, and as a result, the thermal stability of MMLV RT will increase. In the first part of this chapter, we attempted to

increase the thermostability of MMLV RT by introducing positive charges by site-directed mutagenesis at 12 positions (Glu69, Gln84, Asp108, Asp114 Glu117, Glu123, Asp124, Glu286, Glu302, Trp313, Leu435, and Asn454) that have been implicated in the interaction with T/P.

It is generally thought that surface hydrophobic residues decrease protein stability. MMLV RT has five consecutive hydrophobic residues, Leu432-Val433-Ile434-Leu435-Ala436 in the connection domain. Structural analysis revealed that consecutive hydrophobic residues, Phe303-Leu304 and Leu432-Val433-Ile434, are located on the molecular surface (*6*). In the second part of this chapter, we attempted to increase the thermostability of MMLV RT by replacing these surface hydrophobic residues with charged residues.

Materials and Methods

Materials - $p(dT)_{15}$ was purchased from Life Technologies Japan Ltd. (Tokyo, Japan). [methyl-^{3}H]dTTP (1.52 TBq/mmol) and poly(rA) were purchased from GE Healthcare (Buckinghamshire, UK). The glass filter GF/C 2.5 cm is a product of Whatman (Middlesex, UK). RT concentration was determined as according to the method of Bradford (*18*) using Protein Assay CBB Solution (Nacalai Tesque, Kyoto, Japan) with bovine serum albumin (Nacalai Tesque) as a standard. Standard RNA, which was an RNA of 1014-nucleotides corresponding to DNA sequence 8353-9366 of the *cesA* gene of *Bacillus cereus* (GenBank accession number DQ360825), was prepared by *in vitro* transcription (*16*).

Bacterial strains, plasmids, and transformation - *E. coli* BL21(DE3) [F^-, *ompT*, $hsdS_B(r_B^- m_B^-)$ *gal dcm* (DE3)] cells were used. pET-MRT is an expression plasmid for the wild-type MMLV (*12, 19*). Site-directed mutagenesis was carried out using a Quikchange^{TM} site-directed mutagenesis kit (Stratagene, La Jolla, CA). The nucleotide sequences of mutated MMLV RT genes were verified by a Shimadzu DNA sequencer DSQ-2000 (Kyoto, Japan). BL21(DE3) cells were transformed with each of the resulted plasmids and cultured in L broth. Ampicillin was used at the concentration of 50 μg/ml.

Expression and purification of MMLV RT - Three ml of L broth containing 50 μg ml^{-1} ampicillin was inoculated with the glycerol stock of the transformed BL21(DE3) and incubated for 16 h with shaking at 30ºC. The expression of the RT gene was induced by the autoinduction system (Novagen, Darmstadt, Germany). MMLV RT was purified from culture medium using HisLink Spin Protein Purification System (Promega, Madison, WI). Briefly, the bacterial cells were disrupted by FastBreak Cell Lysis Reagent, followed by addition of HisLink Protein Purification Resin to the culture. The samples were then transferred to HisLink Spin Column where unbound protein was washed away. MMLV RT was recovered by the elution with 0.2 ml of 100 mM HEPES-NaOH (pH 7.5), 500 mM imidazole. To the eluted solution, 80% saturated ammonium sulfate solution was added for a final concentration to be 40% saturation. After centrifugation (20,000×g, 20 min), the precipitate was dissolved in 0.5 mM HEPES-NaOH (pH 7.5) and then dialyzed against 20 mM potassium phosphate (pH 7.2), 2 mM DTT, 0.2% Triton X-100, 50% glycerol. MMLV RT thus purified was stored at -80^{o}C before use.

SDS-PAGE - SDS-PAGE was performed in a 10% polyacrylamide gel under reducing conditions according to the method of Laemmli (*20*). Proteins were reduced by treatment with 2.5% of 2-mercaptoethanol at 100ºC for 10 min, and then applied onto the gel. A constant current of 40 mA was applied for 40 min. After electrophoresis, proteins were stained with Coomassie Brilliant Blue R-250. The molecular mass marker kit consisting of rabbit muscle phosphorylase B (97.2 kDa), bovine serum albumin (66.4 kDa), hen egg white ovalbumin (44.3 kDa), and bovine carbonic anhydrase (29.0 kDa) was a product of Takara Bio Inc (Otsu, Japan).

Measurement of the RT activity to incorporate dTTP into poly(rA)-p(dT)$_{15}$ - The reaction was carried out in 25 mM Tris-HCl (pH 8.3), 50 mM KCl, 2 mM DTT, 5 mM $MgCl_2$, 12.5 μM poly(rA)-p(dT)$_{15}$ (this concentration is expressed based on p(dT)$_{15}$), 0.2 mM [^{3}H]dTTP (1.85 Bq/pmol), and 5-10 nM MMLV RT at 37°C. An aliquot (20 μl) was taken from the reaction mixture at a specified time and immediately spotted onto the glass filter. Unincorporated [^{3}H]dTTP was removed by three washes of chilled 5%(w/v) trichloroacetic acid (TCA) for 10 min each, followed by one wash of chilled 95% ethanol. The radioactivity retained on the dried filters was counted in 2.5 ml of Ecoscint H (National Diagnostics, Yorkshire, UK). The initial reaction rate was estimated from the time-course for incorporation of [^{3}H]dTTP. The kinetic parameters, k_{cat} and K_m, were determined with Kaleida Graph Version 3.5 (Synergy Software, Essex, VT), based on the Michaelis-Menten equation and using the non-linear least-squares regression method (*21*).

Thermal inactivation of MMLV RT - MMLV RT (100 nM) in 10 mM potassium

phosphate (pH 7.6), 2 mM DTT, 0.2%(v/v) Triton X-100, 10%(v/v) glycerol was incubated in the presence of 28 μM poly(rA)-p$(dT)_{15}$ at 46-56°C for 0-15 min followed by the incubation on ice for 30-60 min. The remaining activity of the RT toward the incorporation of dTTP into poly(rA)-p$(dT)_{15}$ was determined at 37°C as described above.

Thermodynamic analysis of irreversible thermal inactivation - Assuming that the thermal inactivation reaction of RT is irreversible and consists of only one step, the first-order rate constant, k_{obs}, of the thermal inactivation was evaluated by plotting logarithmic values of the residual activity against the time of heat treatment according to Eq. 1.

$$\ln B = A - k_{obs}\, t \tag{1}$$

where A is the constant term, and B is the relative activity (%) defined as the ratio of the initial reaction rate at a time for the thermal incubation (= t) to that without the incubation. The activation energy, E_a, for the thermal inactivation was determined from an Arrhenius plot according to Eq. 2.

$$\ln(k_{obs}) = A - (E_a/R)(1/T) \tag{2}$$

where A, R, and T are the constant term, the gas constant (= 8.314 J K^{-1} mol^{-1}), and absolute temperature in degrees Kelvin. T_{50} was estimated by Arrhenius plot as the temperature at which the k_{obs} value gives the remaining activity of 50% at 10 min

according to Eq. 1.

Measurement of the RT activity for cDNA synthesis - A standard RNA, which was an RNA of 1014-nucleotides corresponding to DNA sequence 8353-9366 of the *cesA* gene of *Bacillus cereus* (GenBank accession number DQ360825), was prepared by an *in vitro* transcription. The reaction (20 μl) was carried out in 25 mM Tris-HCl (pH 8.3), 50 mM KCl, 2.0 mM DTT, 0.1 mM dNTP, 0.5 μM R12 primer (5'-TGTGGAATTGTGAGCGGTGTCGCAATCACCGTAACACGACGTAG-3'), 0.08 pg/μl standard RNA, 0.05 μg/μl *E. coli* RNA, and 10 nM MMLV RT at a range of temperatures from 46 to 64ºC for 30 min and stopped by heating at 95ºC for 5 min. The PCR reaction mixture (30 μl) was then prepared by mixing water (18 μl), the product of the reverse transcription reaction (3 μl), 10× PCR buffer [500 mM KCl, 100 mM Tris-HCl (pH 8.3), 15 mM MgCl] (3 μl), 10 μM F5 primer (1 μl), of 10 μM RV primer (1 μl), 2.0 mM dNTP (3 μl), and 1 U/μl recombinant *Taq* polymerase (1 μl) (Toyobo, Osaka, Japan). The cycling parameters were 95ºC for 30 s, followed by 30 cycles at 95ºC for 30 s, 55ºC for 30 s, and 72ºC for 30 s. The amplified products were separated on 1.0% agarose gels and stained with ethidium bromide (1 μg/ml). The nucleotide sequences of the primers are shown in Table 1.

Results

1) Stabilization of MMLV RT by introducing positive charges that have been implicated in the interaction with T/P

Design of mutations - Our strategy for increasing the thermal stability of MMLV RT was to increase its binding ability toward the template-primer (T/P) by introducing positive charges into MMLV RT by site-directed mutagenesis at the positions that have previously been implicated in the interaction with T/P. The T/P has phosphate groups and is negatively charged. Based on the crystal structure of the fingers, palm, thumb, and connection domains (Thr24-Pro474) of MMLV RT (*6*), we selected the following 12 residues to be mutated. In the fingers domain (i.e., Thr24-Asp124 and Phe156-Ser195), polypeptide regions Ser60-Gln84, Asn95-Asp124, Phe156-Cys157, and Gln190-Asn194 are located at the surface which interacts with T/P. We thus selected six negatively charged residues (Glu69, Asp108, Asp114 Glu117, Glu123, and Asp124). We also selected Gln84 because site-directed mutagenesis study has identified that Gln84 interacted with T/P (*22*). In the palm domain (i.e., Ile125-Phe155 and Pro196-Glu275), polypeptide regions Ile125-Phe155, Leu220-Glu233, and Lys257-Glu275 are located at the surface which interacts with T/P. However, we did not select any residues because this domain contains the catalytically important residues, Asp224 and Asp225, and mutation might affect their geometries. In the thumb domain (i.e., Gly276-Leu359), residues in polypeptide regions Leu280-Thr287, Arg301-Leu333, and Ala354-Leu359 are located at the surface which interacts with T/P. We selected two negatively charged residues (Glu286 and Glu302). We also selected Trp313 because random mutagenesis studies have identified the mutation Trp313→Phe to increase the stability of MMLV RT (*23*). In the connection domain (i.e., Pro360-Asp468), polypeptide regions Pro360-Lys373, Tyr394-Ala436, and Ser453-Ala462 are located at the surface which interact with T/P. We selected two residues (Leu435 and Asn454)

because random mutagenesis studies have identified the mutations Leu435→Gly, and Asn454→Met to increase the stability of MMLV RT (*23*), while that of Leu435→Lys was identified as improving the solubility of MMLV RT (*17*). Figure 1 shows the locations of these 12 residues in MMLV RT. Each of these was changed either to one of the two positively charged amino acids (Lys and Arg) or to an uncharged one (Ala).

Production of single MMLV RT variants - The 36 variants were expressed in *E. coli* and purified. An RNase H activity-deficient and a stable variant D524A (*12*, *24*) were also prepared. Following SDS-PAGE under reducing conditions, purified WT and variants yielded a single band with a molecular mass of 75 kDa (Figs. 2A-C). The yields of the purified enzymes from 0.7 ml of culture were in the range of 20-74 μg, which were comparable to that of the WT (56 μg). UV absorption spectra of the purified enzymes exhibited the typical UV absorption spectrum of purified protein with a deep trough at about 250 nm and a peak at 275 nm (data not shown). The ratios of the absorbance at 280 nm (A_{280}) to A_{260} of the purified enzymes were in the range of 1.8 to 1.9, indicating that they hardly contained nucleic acids.

Activities and stabilities of single MMLV RT variants - Table 2 shows the specific activities of the reverse transcription reaction for the WT, D524A, and the 36 variants. The specific activity of WT was 70,000 units/mg. All variants can be classified into three groups: (1) The specific activity of D114R was zero; (2) The specific activities of D108K, D108R, D114K, W313K, and W313R were 10-20% of that of WT; and (3) The specific activities of the other 30 variants and D524A were 40-120% of that of WT.

Table 2 also shows the initial reaction rates before and after heat treatment of the

WT, D524A, and all single variants (except for the inactive D114R). Relative activity was defined as the ratio of the initial reaction rate for a 15-min incubation at 50ºC in the presence of T/P to the rate without incubation. The relative activities of WT and D524A were 1.4 and 14%, respectively, which agreed well with those reported in our previous studies (*12, 24*). The relative activity of Q84K was zero, indicating that Q84K was less stable than the WT. The relative activities of the 18 variants (E69A, E69R, D108A, D108K, D108R, E117A, D124K, D124R, E286A, E286K, E286R, E302A, E302K, W313K, W313R, L435A, L435R, and N454R) were in the range of 6-24%, which was substantially higher than that of WT (1.4%). Of these 18, E302K exhibited the highest relative activity (24%), followed by six other variants (E69R, D124K, D124R, E286K, E286R, and L435R) (13-18%).

Activities and stabilities of multiple variants of MMLV RT - To generate highly stable MMLV RT variants, we selected Glu286→Arg, Glu302→Lys, and Leu435→Arg as the mutations to be combined. Glu69→Arg, Asp124→Lys, and Asp124→Arg were not chosen because they decreased the specific activity to 77, 66, and 64%, respectively, of that of WT (Table 2). The RNase H activity-eliminating and stabilizing mutation, Asp524→Ala, was also included in the combination. The resulting triple variant E286R/E302K/L435R (which we termed "MM3") and the quadruple variant E286R/E302K/L435R/D524A (which we termed "MM4") were expressed in *E. coli* and purified. Upon SDS-PAGE under reducing conditions, purified variants yielded a single band with a molecular mass of 75 kDa (Fig. 2D). From 200 ml of cultures, we obtained yields of purified MM3 and MM4 proteins of 410 and 390 μg, respectively.

Table 3 shows the activities and stabilities of MM3 and MM4 proteins. Their

specific activities were 70% of that of WT. Their relative activities after the thermal incubation treatment at 50°C for 15 min were higher than those of WT and D524A, both in the absence and presence of the T/P, indicating that these variant proteins were more stable than the WT and D524A.

Steady-state kinetic analysis - Figure 3 shows the initial reaction rates for 5 nM RT at various T/P concentrations (0-25 μM) at 37ºC. A saturation profile was obtained for Michaelis-Menten kinetics, and the K_m and k_{cat} values were separately determined (Table 4). The K_m values of MM3 and MM4 were 30 and 40% of that of WT, respectively, while their k_{cat} values were 40 and 50% of that of WT, respectively. The k_{cat}/K_m values of MM3 and MM4 were 170 and 130% of that of WT.

Irreversible thermal inactivation of MMLV RT - The remaining reverse transcription activities of WT and the multiple variants were determined at 37ºC after thermal treatment in the presence of the T/P. The WT and D524A were treated at 48-52ºC, while MM3 and MM4 were treated at 52-58ºC. The natural logarithm of the remaining activity plotted against the incubation time gave linear relationships at 52ºC (Fig. 4A) and at all other temperatures examined (data not shown), indicating that the inactivation followed pseudo-first-order kinetics. The relative activity of WT decreased to less than 10% at 5 min. The relative activity of D524A decreased more slowly than did WT, but decreased to 20% at 5 min. The relative activities of MM3 and MM4 decreased only slightly, indicating that they were much more stable than WT and D524A.

Figure 4B shows an Arrhenius plot of k_{obs} of the thermal inactivation of RT in the

presence of the T/P. The natural logarithm of k_{obs} and $1/T$ showed a linear relationship. The temperatures required to reduce initial activity by 50% over a 10-min incubation (T_{50}) were 45, 48, 54, and 56ºC for the WT, D524A, MM3 and MM4, respectively, as estimated from the Arrhenius plot, indicating that the stabilities were in the order of MM4 > MM3 > D524A > WT. The activation energies (E_a) of thermal inactivation of WT, D524A, MM3, and MM4, as calculated from the slope, showed a close similarity at 241 ± 46, 279 ± 15, 298 ± 42, and 322 ± 22 kJ mol^{-1}, respectively.

MMLV RT-catalyzed cDNA synthesis - The cDNA synthesis reaction was carried out with WT and the variants at 44-64°C. The reaction product was subjected to PCR, followed by agarose gel electrophoresis, to determine the rate of cDNA synthesis at specific temperatures (Fig. 5). The highest temperatures at which cDNA synthesis occurred were 54, 56, 60, and 60°C, for the WT, D524A, MM3, and MM4, respectively. This indicated stability in the order of MM3 and MM4 > D524A > WT.

2) Stabilization of MMLV RT by replacing surface hydrophobic residues with charged residues

Production of single MMLV RT variants – To advance further stabilization of MMLV RT, we mutated it with another strategy. On the assumption that MMLV RT stability increases upon introduction of the charged residue into one of these consecutive surface hydrophobic residues (Fig. 6), 10 variants (F303R, F303K, L304R, L304K, L432R, L432K, V433R, V433K, I434R, and I434K) were constructed in which one of these five residues was replaced with Arg or Lys. C-terminally $(His)_6$-tagged

variants were expressed in *E. coli* and purified from the cells by a method described previously (*25*). Following SDS-PAGE under reducing conditions, the purified enzyme preparations yielded a single band with a molecular mass of 75 kDa (Fig. 7A).

Activities and stabilities of single MMLV RT variants - Figure 7B shows the specific activities of the reverse transcription reaction for WT and all the single variants. All the variants were classifiable into three groups: (i) The specific activities of L304R and L304K were close to zero; (ii) the specific activities of L432R and I434R were 40−60% of that of WT; and (iii) the specific activities of the other six variants were 80−100% of that of WT. Figure 7C shows the relative activities of WT and all single variants except for L304R and L304K, the activities of which were markedly reduced. Relative activity was defined as the ratio of the reaction rate for 10 min incubation at 48 or 50ºC in the presence of T/P to the rate without incubation. All variants were classifiable into two groups: (i) The relative activities of V433R and V433K were 3−5 fold higher than that of WT and (ii) the relative activities of other six variants were similar to that of WT.

Activities and stabilities of multiple variants of MMLV RT - It is generally thought that if mutated sites are not in contact, the chances that mutational effects will be additive are high (*26*). Indeed, we generated highly stable MMLV RT variants MM3 and MM4 by the combination of mutations. Therefore, we selected Val433→Arg as the mutations to be combined. Figure 8 shows the relative activities of WT and variants for incubation at 50ºC for 10 min in the presence of T/P. Relative activities increased with increasing numbers of mutations combined to Val433→Arg, and reached 70% for

D108R/E286R/V433R (which we termed "MM7") and D108R/E286R/V433R/D524A (which we termed "MM8"), indicating that the effects of the stabilizing mutations were additive. As Fig. 8 also indicates, the stabilities of MM7 and MM8 were similar to those of MM3 and MM4. The specific activities of the enzyme preparations were 31,000 units/mg for MM3, 35,000 units/mg for MM4, 33,000 units/mg for MM7, and 25,000 units/mg for MM8, almost the same.

Discussion

Stabilization of MMLV RT by introducing basic residues into the template-primer binding site - Our hypothesis that the thermal stability of MMLV RT increases when binding ability for the template-primer (T/P) increases is based on the evidence that T/P increases the thermal stabilities of MMLV RT and AMV RT (*13, 14*). A number of variants exhibited higher stability than WT (Table 2); some exhibited even higher stability than D524A, a known stable variant. Therefore, our strategy appeared to be effective for stabilizing MMLV RT. However, mutations at Asp108 or Asp114 decreased the activity, while those at Gln84 decreased the stability. In the fingers domain of MMLV RT (i.e., Thr24-Asp124 and Phe156-Ser195), the Lys103, Arg110, and Arg116 are conserved in HIV-1 RT, AMV RT, and the Klenow fragment, and are thought to provide the binding site for T/P (*27*). We speculate that mutations at Gln84, Asp108, or Asp114 affected the geometries of the regions around Lys103, Arg110, or Arg116, resulting in decreased activity or stability.

Affinity of MMLV RT for T/P following introduction positive charges into the

template-primer binding site - The relative activities of MM3 and MM4 were higher in the presence of T/P than in its absence (Table 3). The K_m values for T/P of the MM3 and MM4 were 20-30% of that of WT (Table 4). Thus, the affinities of the multiple variants for T/P were apparently higher than WT affinity. However, even in the absence of the T/P, the relative activities of MM3 and MM4 were higher than that of WT (Table 3). This suggests that the increased stability of MM3 and MM4 resulted from an increased affinity for T/P and also an increased intrinsic stability.

It was recently reported that five stabilizing mutations (Glu69→Lys, Glu302→Arg, Trp313→Phe, Leu435→Gly, and Asn454→Lys) were developed by random mutagenesis, and that a highly stable multiple variant E69K/E302R/W313F/L435G/N454K (M5) was generated (*23*). Some of the substituted residues in M5 (Glu302 and Leu435) are overlapped with the triple and quadruple variants presented in this study. Interestingly, M5 was stabilized in the presence of the T/P, but not in its absence (*23*). This suggests that unlike MM3 and MM4, the increased stability of M5 resulted from an increased affinity for T/P, but not from an increased intrinsic stability. We speculate that the mechanism of stabilization of M5 is different from that of MM3 and MM4, although both in M5 and the multiple variants, the number of negatively charged residues (Asp and Glu) decreased by two, and the number of positively charged residues (Lys and Arg) increased by three compared to WT.

Stabilization of MMLV RT by introducing the combined stabilizing mutations, Glu286→Arg, Glu302→Lys, and Leu435→Arg - Site-directed mutagenesis and/or random mutations have been extensively performed for a number of enzymes, and mutations have been identified that confer desirable properties to the enzymes. When

the effects of these mutations are additive, a variant enzyme with multiple mutations would be expected to show more desirable properties. According to a summary of characterization of about 700 variants of phage T4 lysozyme, various kinds of effective stabilizing processes can occur, such as S-S bridges, salt-bridge interactions, metal binding, and hydrophobic stabilization. If the mutated sites are on the molecular surfaces that are not in contact, the stabilizing effects will be additive (*26*). On the other hand, a compromise between activity and stability is generally recognized in various enzymes: mutations that increase enzyme activity also decrease protein stability, while those that increase protein stability decrease enzyme activity (*28-33*). In addition, predicting the effect of mutational combination on enzyme properties is not a simple matter.

The relative activity of WT was 1.4% in the presence of T/P (Table 2). The individual mutations, Glu286→Arg, Glu302→Lys, Leu435→Arg, and Asp524→Ala, increased this to 15, 24, 18, and 14%, respectively (Table 2). When the first three mutations were combined, the relative activity increased to 82%; while combination of all four mutations increased it to 101% (Table 3), indicating an additive effect of these mutations on stability. On the other hand, the combination of Glu286→Arg, Glu302→Lys, and Leu435→Arg decreased the specific activity to 67-69% of that of WT, although each individual mutation did not (Table 2). In this case, the stabilizing effects of the mutations were additive, but the combination resulted in a slight decrease in activity.

cDNA synthesis by the highly stable multiple variants - The triple and quadruple variants exhibited cDNA synthesis activity at a highest temperature of 60^{o}C, which was

higher than that seen for WT (54ºC) or D524A (56ºC) (Fig. 5). These variants may therefore be useful for cDNA synthesis reactions. The degree of stability was similar to that reported previously for the stable MMLV RT variant E69K/E302R/W313F/L435G/N454K/D524N (*23*).

We previously examined the effects of organic solvents on cDNA synthesis catalyzed by MMLV RT, and showed that glycerol increased the thermal stability of MMLV RT and AMV RT (*34*). Like glycerol, the disaccharide trehalose increases the thermal stability of MMLV RT (*35*). Glycerol and trehalose are widely used in the storage of thermolabile enzymes. However, the theory underlying thermal stabilization by sugars such as glycerol and trehalose has not yet been established. Whether glycerol and trehalose can further increase the thermal stabilities of our triple and quadruple variants will be the subject of our next investigations. In regard of this, it was recently reported that the stable MMLV RT variant, M5 is highly resistant to common RT-PCR inhibitors including guanidine, thiocyanate, ethanol, formamide, ethylenediaminetetraacetic acid (EDTA), and plant-related acidic polysaccharides (*36*).

Stability of MMLV RT following introduction of positive charges into a hydrophobic surface of the RT - MMLV RT is an unstable enzyme. It aggregates easily. In this study, all purification procedures were conducted at 4°C in the presence of 2.0 mM DTT and 10% v/v glycerol, and storage was done at −80°C in the presence of 2.0 mM DTT and 50% glycerol. It is generally thought that two steps, the formation of intermolecular disulfide bonds and intermolecular interaction of hydrophobic surfaces, are important in protein aggregation. We think that the stabilizing effects of Val433→Arg and Val433→Lys result from a decrease in the interaction of hydrophobic

surfaces. Thus V433R and V433K aggregate less easily than WT. Regarding this, we have found that glycerol inhibited the inactivation of MMLV RT during incubation at 43°C (*34*). Glycerol is an osmolyte that reduces the water activity of the solution. It stabilizes proteins and folds denatured proteins correctly (*37*). Such a high glycerol concentration does not cause any problem in use of MMLV RT in cDNA synthesis, but does for physico-chemical analysis of MMLV RT. We speculate that the mechanisms of the effects of glycerol and mutation Val433→Arg on MMLV RT stability are similar. If this is true, the glycerol concentration required to minimize aggregation can be reduced for variants with mutation Val433→Arg. As for the fidelity of reverse transcription, we think that Val433→Arg and Val433→Lys have no effect on it, because the active site of DNA polymerase reaction resides in the fingers/palm/thumb domain, not in the connection subdomain in which Val433 is located.

In conclusion, four highly stable MMLV RT variants, MM3, MM4, MM7, and MM8 were generated by combining various stabilizing mutations. These multiple variants, as well as others previously reported, might be useful not only for elucidating the structure-function relationship of MMLV RT but also in research and diagnostic applications involving cDNA synthesis and RNA-specific amplification.

Table 1. Primers.

Primers	Sequences (5'-3')
RV-R26[a]	*TGTGGAATTGTGAGCGG*TGTCGCAATCACCGTAACACGACGTAG
F5[b]	TGCGCGCAAAATGGGTATCAC
RV	TGTGGAATTGTGAGCGG

The mismatched nucleotides with the sequence of the wild-type MMLV RT are underlined.

[a]The italicized sequence is identical with that of RV primer, and that underlined corresponds to 9308-9333 of the sequences deposited in GenBank (DQ360825).

[b]The underlined sequence corresponds to 8725-8745 of the sequences deposited in GenBank (DQ360825).

Table 2. Activity and stability of the single variants.

	Specific activity [a] (units/mg)	Initial reaction rate (nM/s)	
		Before heat treatment [b]	After heat treatment with T/P [c]
WT	70,000 (1.00) [d]	41.8	0.59 (0.014) [e]
D524A	68,000 (0.97)	40.6	5.68 (0.14)
E69A	74,000 (1.06)	44.5	3.37 (0.076)
E69K	73,000 (1.04)	43.9	0.07 (0.002)
E69R	54,000 (0.77)	32.6	4.19 (0.13)
Q84A	84,000 (1.20)	50.1	0.46 (0.009)
Q84K	59,000 (0.84)	35.1	0 (0)
Q84R	68,000 (0.97)	40.9	0.29 (0.007)
D108A	69,000 (0.99)	41.5	2.58 (0.062)
D108K	14,000 (0.20)	8.7	0.92 (0.11)
D108R	12,000 (0.17)	7.2	0.74 (0.10)
D114A	42,000 (0.60)	25.4	0.10 (0.004)
D114K	6,000 (0.09)	3.3	0.01 (0.004)
D114R	0 (0)		
E117A	67,000 (0.96)	40.2	2.65 (0.066)
E117K	32,000 (0.46)	19.4	0.56 (0.029)
E117R	51,000 (0.73)	30.7	0.29 (0.009)
E123A	76,000 (1.09)	45.6	0.82 (0.018)
E123K	77,000 (1.10)	46.0	0.28 (0.006)
E123R	67,000 (0.96)	40.5	0.08 (0.002)
D124A	71,000 (1.01)	42.6	1.47 (0.034)
D124K	46,000 (0.66)	27.7	4.33 (0.16)
D124R	45,000 (0.64)	27.1	4.51 (0.17)
E286A	71,000 (1.01)	42.6	5.12 (0.12)
E286K	63,000 (0.90)	37.6	5.90 (0.16)
E286R	71,000 (1.01)	42.6	6.48 (0.15)
E302A	66,000 (0.94)	39.7	3.97 (0.10)
E302K	67,000 (0.96)	40.1	9.67 (0.24)
E302R	69,000 (0.99)	41.3	0.87 (0.002)
W313A	27,000 (0.39)	16.1	0.63 (0.039)
W313K	5,000 (0.07)	3.0	0.32 (0.11)
W313R	5,000 (0.07)	2.9	0.22 (0.074)
L435A	61,000 (0.87)	36.3	3.56 (0.098)
L435K	75,000 (1.07)	45.1	1.17 (0.026)
L435R	65,000 (0.93)	39.2	6.95 (0.18)
N454A	67,000 (0.96)	40.1	1.56 (0.039)
N454K	76,000 (1.09)	45.6	0.50 (0.011)
N454R	60,000 (0.86)	38.0	2.81 (0.074)

The average of triplicate determination is shown for WT and D524A, and that of duplicate determination is shown for the other variants.

[a, b]The reaction was carried out in 10 nM RT, 25 mM Tris-HCl (pH 8.3), 50 mM KCl, 2 mM DTT, 5 mM $MgCl_2$, 25 μM poly(rA)-$p(dT)_{15}$ (this concentration is expressed based on $p(dT)_{15}$), and 0.4 mM [^{3}H]dTTP at 37ºC. One unit is defined as the amount which incorporates 1 nmol of dTTP into poly(rA)-$p(dT)_{15}$ in 10 min.

[c]RT at 100 nM was incubated at 50ºC in the absence or presence of poly(rA)-$p(dT)_{15}$ (28 μM) for 15 min. Then, the dTTP incorporation reaction was carried out at 37°C.

[d]Numbers in parentheses indicate values relative to WT.

[e]Numbers in parentheses indicate the relative activity, which is defined as the ratio of the initial reaction rate with incubation to that without incubation.

Table 3. Activity and stability of the multiple variants.

	Specific activity [a] (units/mg)	Initial reaction rate (nM/s)		
		Before heat treatment [b]	After heat treatment without T/P [c]	After heat treatment with T/P [d]
WT	70,000 ± 1,000 (1.00) [e]	41.8 ± 0.6	0.08 ± 0.03 (0.002) [f]	0.59 ± 0.38 (0.014)
D524A	68,000 ± 9,000 (0.97)	40.6 ± 5.4	1.13 ± 0.16 (0.028)	5.68 ± 0.41 (0.14)
MM3	47,000 ± 2,000 (0.67)	28.1 ± 1.2	6.74 ± 0.03 (0.24)	23.0 ± 5.1 (0.82)
MM4	48,000 ± 6,000 (0.69)	28.7 ± 3.6	9.76 ± 0.29 (0.34)	29.0 ± 0.3 (1.01)

The average of triplicate determination with SD values is shown.

[a, b]The experimental condition and the unit definition correspond to those of Table 2. Molecular masses used for the calculation are 72,161, 72,117, 72,230, and 72,186 Da for WT, D524A, MM3, and MM4, respectively.

[c, d] RT at 100 nM was incubated at 50ºC in the absence[c] or presence[d] of poly(rA)-p$(dT)_{15}$ (28 μM) for 15 min. Then, the dTTP incorporation reaction was carried out at 37°C.

[e]Numbers in parentheses indicate values relative to WT.

[f]Numbers in parentheses indicate the relative activity, which is defined as the ratio of the initial reaction rate with incubation to that without incubation.

Table 4. Kinetic parameters of the wild-type MMLV RT and the variants in the reverse transcription reaction at 37°C.

	K_m (μM)	k_{cat} (s^{-1})	k_{cat}/K_m (μM^{-1} s^{-1})
WT	8.4 ± 2.0 (1.0)	13.0 ± 1.2 (1.0)	1.5 ± 0.2 (1.0)
D524A	5.2 ± 1.2 (0.6)	9.2 ± 0.7 (0.7)	1.8 ± 0.3 (1.2)
MM3	2.2 ± 1.1 (0.3)	5.6 ± 0.6 (0.4)	2.5 ± 1.1 (1.7)
MM4	3.3 ± 0.7 (0.4)	6.6 ± 0.4 (0.5)	2.0 ± 0.3 (1.3)

The average of triplicate determination with SD values is shown. Numbers in parentheses indicate values relative to WT.

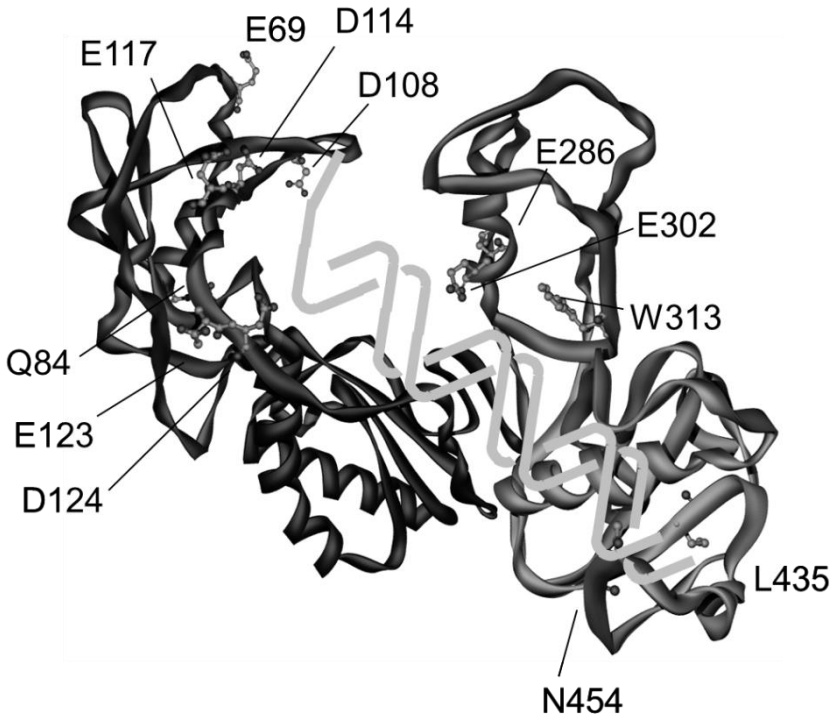

Fig. 1. Overall structure of MMLV RT. The structure is based on Protein Data Bank number 1RW3 (*6*). Peptide chain is displayed by a ribbon model. Residues subject to mutation are displayed by ball and stick. Template-primer (T/P) is schematically shown based on its presumed trajectory exiting the polymerase active site of MMLV RT (*6*).

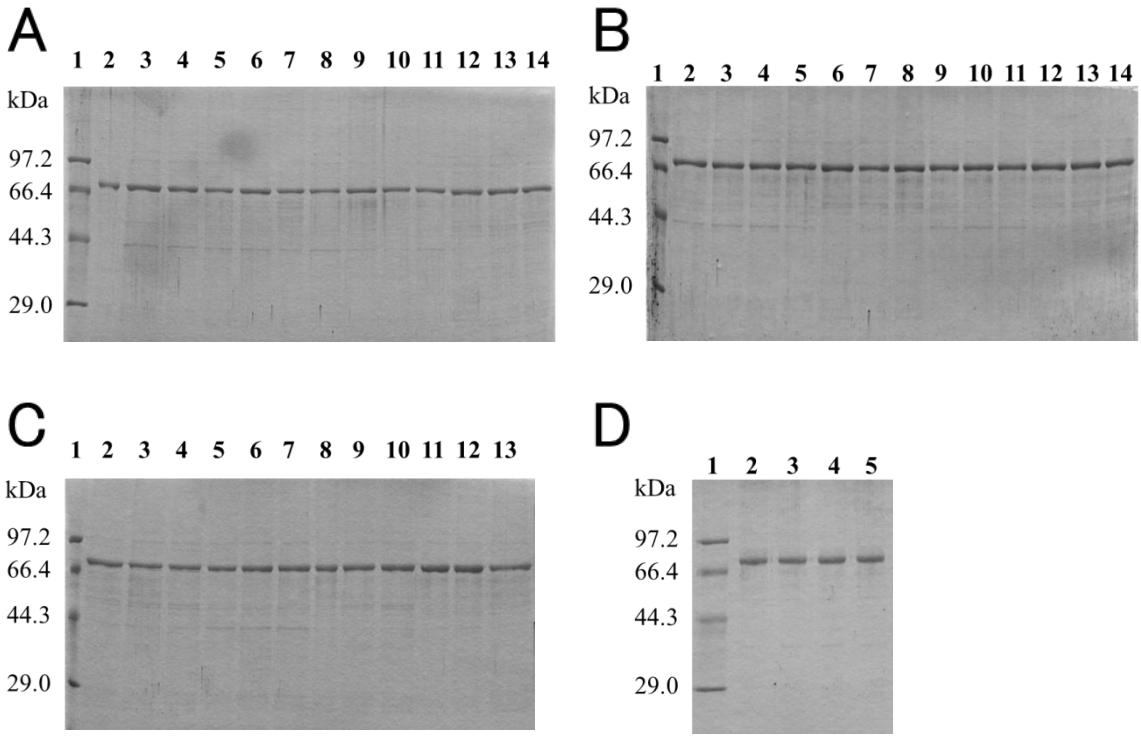

Fig. 2. SDS-PAGE of MMLV RT variants under reducing conditions. One μg protein was applied to each lane. Coomassie Brilliant Blue-stained 10% SDS-polyacrlamide gels is shown. (A) Lane 1, molecular-mass marker; lane 2, the wild-type MMLV RT (WT), lane 3, E69A; lane 4, E69K; lane 5, E69R; lane 6, Q84A; lane 7, Q84K; lane 8, Q84R; lane 9, D108A; lane 10, D108K; lane 11, D108R; lane 12, D114A; lane 13, D114K; lane 14, D114R. (B) Lane 1, molecular-mass marker; lane 2, D524A; lane 3, E117A; lane 4, E117K; lane 5, E117R; lane 6, E123A; lane 7, E123K; lane 8, E123R; lane 9, D124A; lane 10, D124K; lane 11, D124R; lane 12, E286A; lane 13, E286K; lane 14, E286R. (C) Lane 1, molecular-mass marker; lane 2, E302A; lane 3, E302K; lane 4, E302R; lane 5, W313A; lane 6, W313K; lane 7, W313R; lane 8, L435A; lane 9, L435K; lane 10, L435R; lane 11, N454A; lane 12, N454K; lane 13, N454R. (D) Lane 1, molecular-mass marker; lane 2, WT; lane 3, D524A; lane 4, MM3; lane 5, MM4.

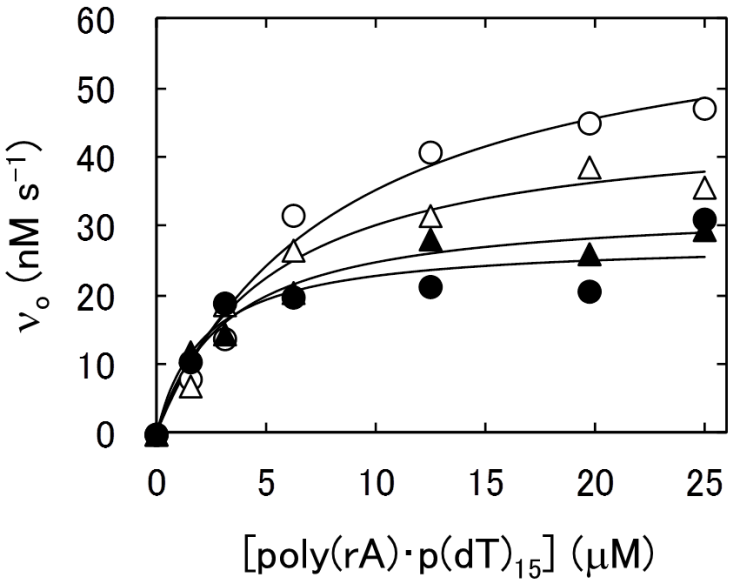

Fig. 3. Dependence on substrate concentration of the initial reaction rate of RT-catalyzed incorporation of dTTP into poly(rA)-p(dT)$_{15}$ at 37ºC. The initial concentrations of RT and dTTP were 5 nM and 200 μM, respectively. Solid lines represent the best fit of the Michaelis-Menten equation with the non-linear least squares method. Symbols for the enzymes: WT, open circle; D524A, open triangle; MM3, closed circle; MM4, closed triangle.

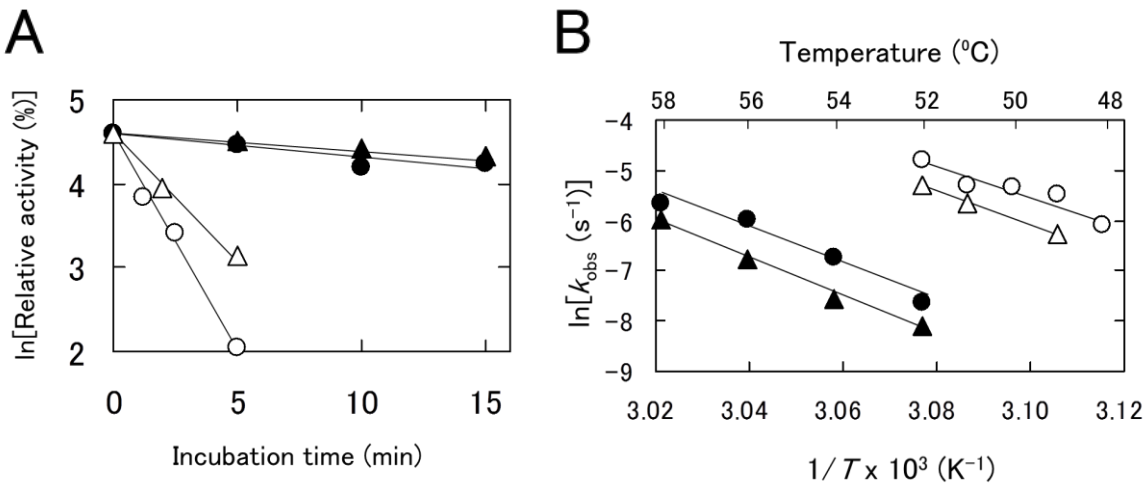

Fig. 4. Irreversible thermal inactivation of MMLV RT. RT at 100 nM was incubated at 48-58ºC in the presence of poly(rA)-p(dT)$_{15}$ (28 μM) for the indicated durations. Then, the reverse transcription reaction was carried out at 37°C. The relative activity of RT was defined as the ratio of the initial reaction rate with incubation for the indicated durations to that without incubation [25 nM s^{-1} for WT (5 nM), 26 nM s^{-1} for D524A (5 nM), 29 nM s^{-1} for MM3 (10 nM), and 33 nM s^{-1} for MM4 (10 nM)]. (A) Irreversible thermal inactivation at 52ºC. The first-order rate constant of the thermal inactivation (k_{obs}) of RT was estimated from the slope: WT (open circle), 8.3×10^{-3} s^{-1}; D524A (open triangle), 6.0×10^{-3} s^{-1}; MM3 (closed circle), 4.9×10^{-4} s^{-1}; MM4 (closed triangle) 3.0×10^{-4} s^{-1}. (B) Arrhenius plot of k_{obs} values. The activation energy (E_a) of thermal inactivation with the T/P of RT was calculated from the slope: WT (open circle), 241 ± 46 kJ mol^{-1}; D524A (open triangle), 279 ± 15 kJ mol^{-1}; MM3 (closed circle), 298 ± 42 kJ mol^{-1}; MM4 (closed triangle), 322 ± 22 kJ mol^{-1}.

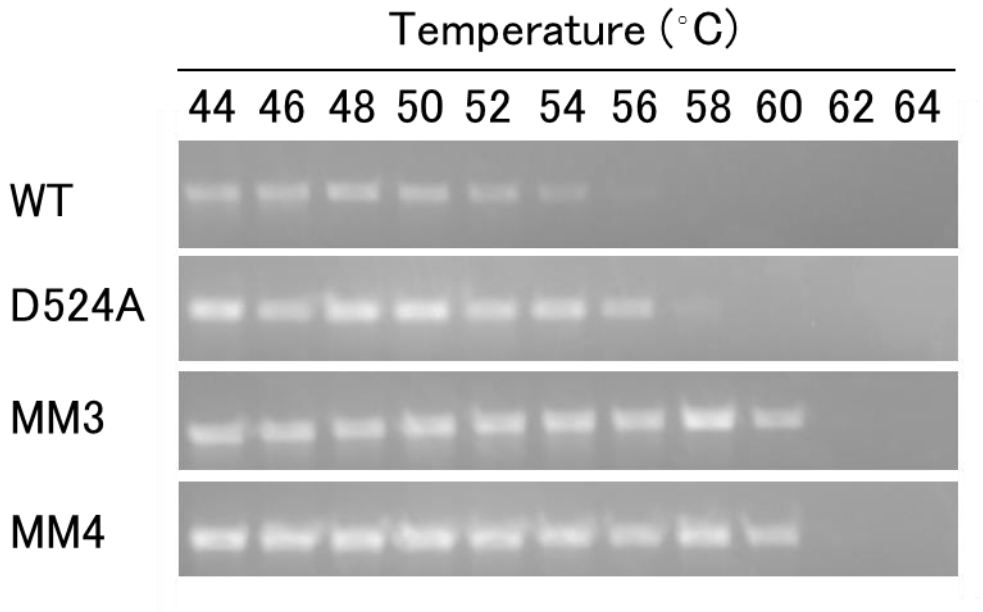

Fig. 5. Dependence on reaction temperature of cDNA synthesis. cDNA synthesis was carried out with 1.6 pg *cesA* RNA, 0.2 μM RV-R26 primer, and 10 nM RT at 44-64ºC for 30 min. PCR was carried out with a primer combination of RV and F5. Amplified products were applied to 1% agarose gel followed by staining with ethidium bromide (1 μg/ml).

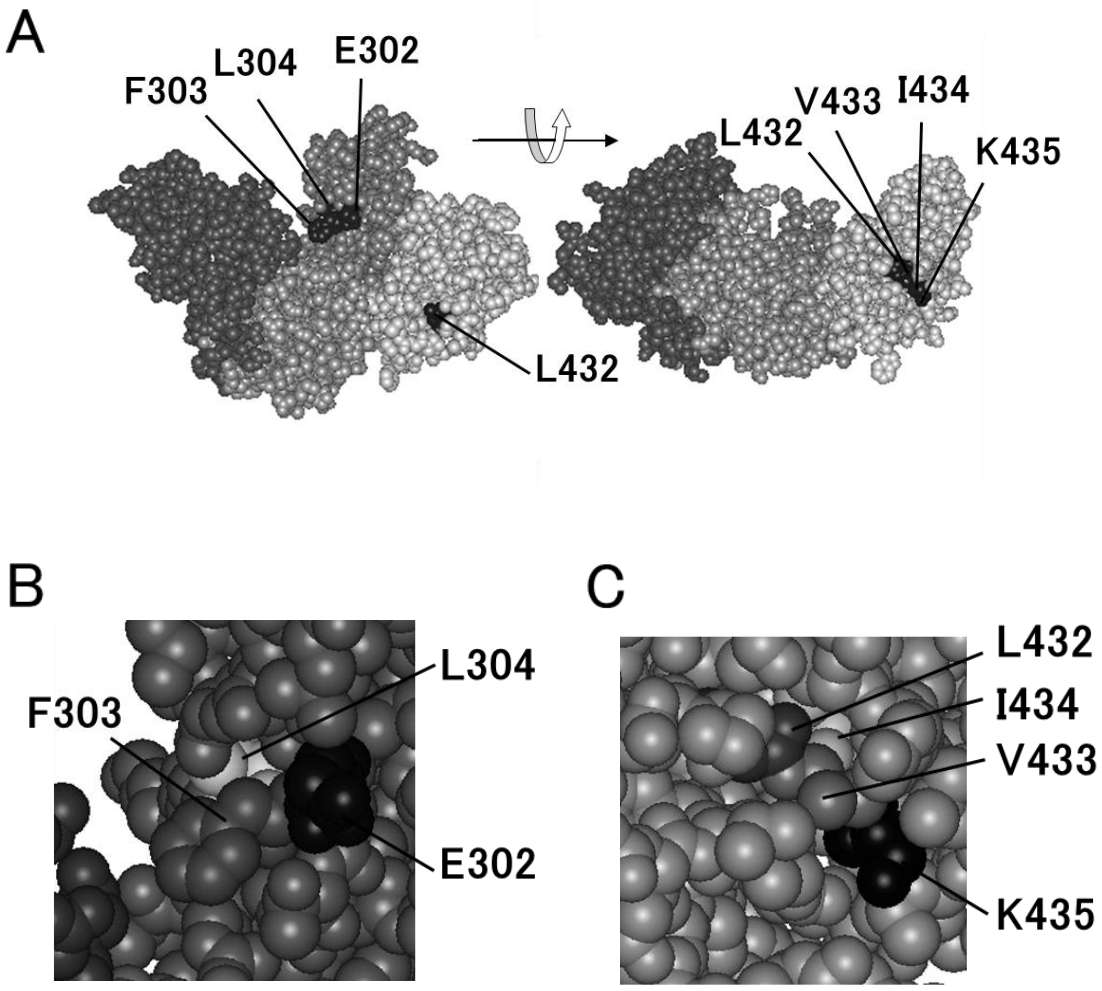

Fig. 6. Structure of MMLV RT variant L435K. The structure is based on Protein Data Bank no. 1RW3. (A) Overall structure. (B) Close-up view of the surface region, in which Phe303 and Leu304 are located. (C) Close-up view of the surface region, in which Leu432, Val433, and Ile434 are located.

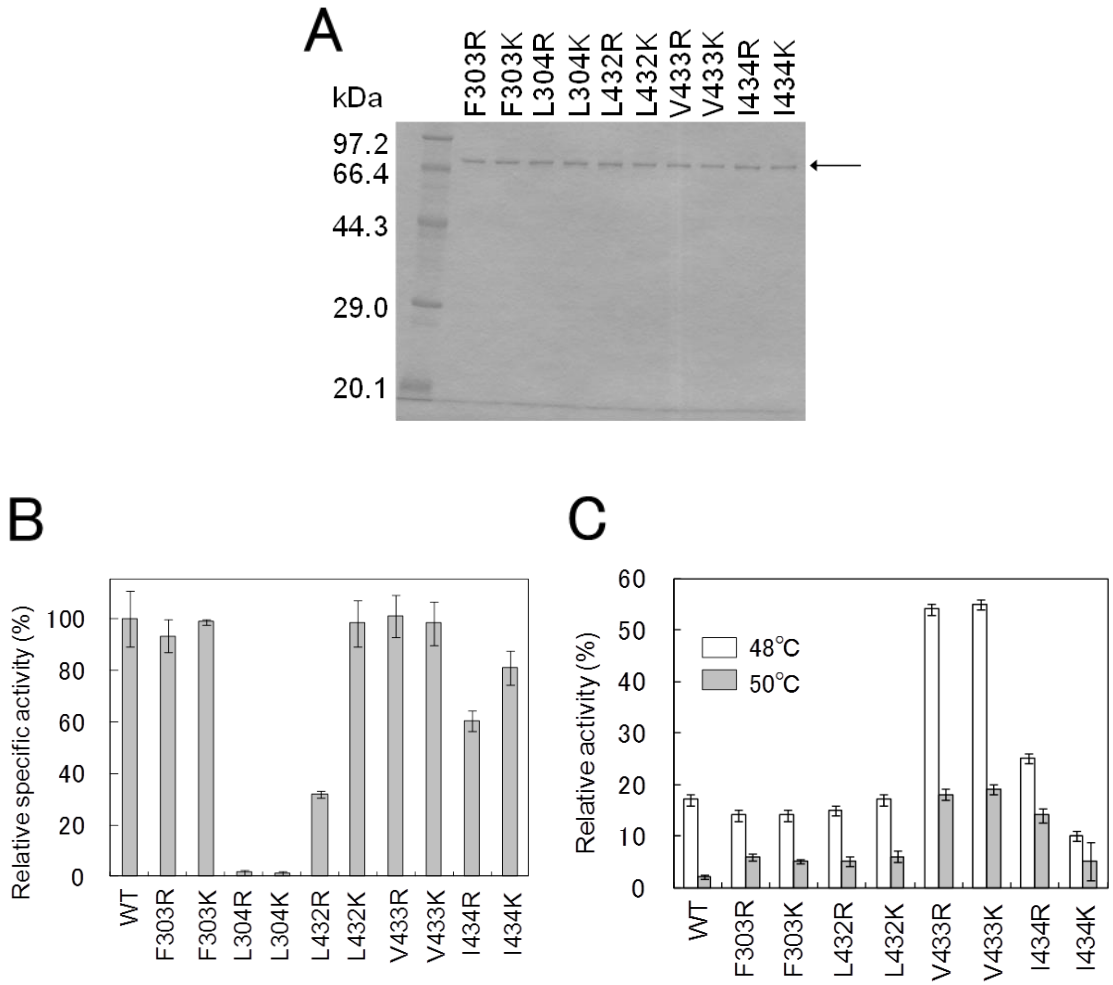

Fig. 7. Analysis of single MMLV RT variants. (A) SDS-PAGE under reducing conditions. Coomassie Brilliant Blue-stained 10% SDS-polyacrlamide gels is shown. The arrow indicates the band corresponding to MMLV RT. (B) Specific activity. One unit was defined as the amount that incorporates 1 nmol of dTTP into poly(rA)-p$(dT)_{15}$ in 10 min. Relative specific activity was defined as the ratio of the specific activity of RT to that of WT (34,000 units/mg). (C) Thermal stability. RT at 50 nM was incubated at 48 or 50ºC for 10 min. Then a dTTP incorporation reaction was carried out at 37°C. Relative activity was defined as the ratio of the initial reaction rate of RT with 10 min incubation at 48 or 50°C to that without the incubation.

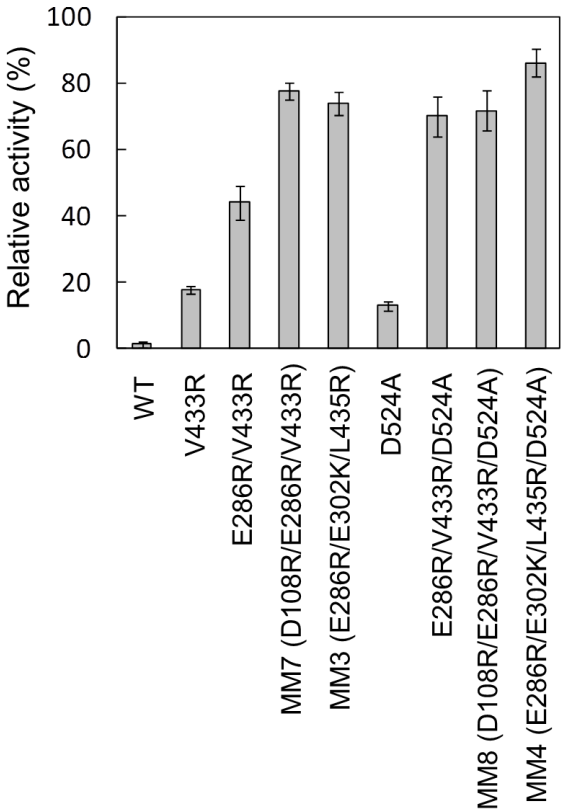

Fig. 8. Thermal stability of multiple MMLV RT variants. RT at 50 nM was incubated with 28 μM poly(rA)-p$(dT)_{15}$ at 50ºC for 10 min. Then a dTTP incorporation reaction was carried out at 37°C. Relative activity was defined as the ratio of the initial reaction rate of RT with 10 min incubation at 50°C to that without incubation.

Chapter 2

Thermostabilization of avian myeloblastosis virus reverse transcriptase by site-directed mutagenesis

Introduction

As described in General Introduction, like MMLV RT, the thermostability of AMV RT is low: the initial reverse transcriptase activities of AMV RT in the absence and presence of T/P are reduced by 50% at 47 and 52ºC, respectively, during a 10-min incubation (*12*). Thus, generation of thermostable AMV RT is also an important subject. In AMV RT, natural enzymes purified from blood of AMV-infected chicken have been used in cDNA synthesis because, unlike recombinant MMLV RT (*38, 39*), recombinant AMV RT has barely been expressed in soluble fractions in *E. coli*. Crystal structure of AMV RT is not available.

Considering that the sequence homology between AMV RT and MMLV RT is 23%, we hypothesized that the results obtained in Chapter 1 is applicable to stabilize AMV RT. Sequence comparison reveals that Glu286, Glu302, Leu435, and Asp524 of MMLV RT correspond to Val238, Lys254, Leu388, and Asp450, respectively, of AMV RT (Fig. 1). To test the hypothesis, in the first part of this chapter, we attempted to establish a new method for the production of AMV RT by using insect cells. In the second part of this chapter, using the insect expression system for AMV RT α subunit

we established, we attempted to increase the thermostability of AMV RT α subunit by introducing the mutations, V238→R, L388→R, D450→A, which were comparable to the stabilizing mutations of MMLV RT (Chapter 1).

Materials and methods

Expression in insect cells of AMV RT α subunit - pFastBac1 (Invitrogen, Carsbad, CA) was digested by *Bam*HI and *Eco*RI. Oligonucleotides 5'-GATCTCCGGTCATATGCGCGCGG-3' and 5'-AATTCCGCGCGCATATGACCGGA-3' were annealed and inserted in it to disrupt the *Bam*HI site and introduce the *Nde*I site. pET-ARTα (*19*) was used as a template for PCR. The 1,758-bp fragment containing the gene for the C-terminally $(His)_6$-tagged AMV RT α subunit was amplified using oligonucleotides 5'-AAGGAGATATACATATGACTGTTGCGCTACA-3' and 5'-CTGAATTCTAGTGGTGATGGTGGTGGTGATACGCTTGAAAGGTGG-3', digested by *Nde*I, and inserted in the above plasmid digested by *Nde*I and *Eco*RI, to give pFastBac1-ARTα (Fig. 2A). *E. coli* DH10Bac (Invitrogen), which contains a baculovirus shuttle vector (bacmid) and a helper plasmid, was transformed with pFastBac1-ARTα. Sf9 insect cells (Invitrogen) were grown in IPL-41 medium (Invitrogen) containing 3.5% fetal bovine serum at 28°C. The recombinant bacmid was prepared from the transformed DH10Bac cells and transfected into Sf9 cells. After preparation of the first virus stock solution, two rounds of infection were performed to amplify the virus titer. For expression of the AMV RT α subunit, 100 ml of Sf9 cells at a

density of 1×10^6 cells/ml was infected with recombinant baculovirus and cultivated in IPL-41 medium containing 3.5% fetal bovine serum for 120 h at 28°C. After cultivation, the cells were harvested by centrifugation (15,000 × *g*, 20 min).

Purification of AMV RT α subunit - The purification step comprised ammonium sulfate fractionation, anion-exchange chromatography, and Ni^{2+} affinity chromatography. All procedures were conducted within 2 d at 4°C. The harvested cells were suspended with 20 ml of 10 mM Tris-HCl (pH 7.5), 0.4% Triton X-100, 10% glycerol, and 1.0 mM phenylmethanesulfonyl fluoride (buffer A), and were disrupted by sonication. After centrifugation at 15,000 × *g* for 20 min, the supernatant was collected, and solid $(NH_4)_2SO_4$ was added to a final concentration of 40% saturation. After centrifugation at 20,000 × *g* for 20 min, the pellet was collected and dissolved in 6 ml of 20 mM potassium phosphate, 2.0 mM DTT, 2.0% Triton X-100, and 10% glycerol pH 7.2 (buffer B), and dialyzed against the same buffer. The solution was added to 54 ml of 2.0 mM DTT, 2.0% Triton X-100, and 10% glycerol pH 7.2, and applied to the column (10 mm inner diameter × 30 mm) packed with DEAE650M (Tosoh, Tokyo) equilibrated with buffer B. The fractions containing the AMV RT α subunit were eluted with 300 mM potassium phosphate, 2.0 mM DTT, 2.0% Triton X-100, and 10% glycerol pH 7.2 and dialyzed against buffer B containing 20 mM imidazole. The solution was applied to the column packed with Ni^{2+}-Sepharose (HisTrap HP 1 ml, GE Healthcare, Buckinghamshire, UK) equilibrated with the same buffer. The column was washed with buffer B containing 50 mM imidazole first and buffer B containing 80 mM imidazole secondly. The bound α subunit was eluted with buffer B containing 500 mM imidazole. The eluate was dialyzed against 20 mM potassium phosphate, 2.0 mM DTT, 0.2%

Triton X-100, and 50% glycerol pH 7.2, and stored at -80°C. The RT concentration was determined by the method of Bradford (*18*) using Protein Assay CBB Solution (Nacalai Tesque, Kyoto) with bovine serum albumin as standard. Starting with 100 ml of culture, about 20 μg of the purified α subunit was recovered. On SDS-PAGE under reducing conditions, the α subunit preparation thus obtained yielded a single band with a molecular mass of 63 kDa (Fig. 2B).

Measurement of AMV RT activity to incorporate dTTP into poly(rA)-p(dT)$_{15}$ - The activity of AMV RT to incorporate dTTP into poly(rA)-p(dT)$_{15}$ was performed as described previously (*34*). Briefly, the reaction was carried out in 25 mM Tris-HCl (pH 8.3), 50 mM KCl, 2.0 mM DTT, 5.0 mM $MgCl_2$, 25 μM poly(rA)-p(dT)$_{15}$ (this concentration expressed as that of p(dT)$_{15}$), 0.4 mM [^{3}H]dTTP, and 10% (v/v) samples at 37ºC. An aliquot (20 μl) was taken from the reaction mixture at a predetermined time and immediately spotted onto the glass filter GF/C 2.5 cm (Whatman, Middlesex, UK). The amounts of [^{3}H]dTTP incorporated was counted, and the initial reaction rate was determined. The kinetic parameters, Michaelis constant (K_m) and molecular activity (k_{cat}), were determined with Kaleida Graph Version 3.5 (Synergy Software, Essex, VT).

Irreversible thermal inactivation of AMV RT – Thermal inactivation of AMV RT was performed as described in Chapter 1.

Thermodynamic analysis of thermal inactivation of AMV RT - The thermodynamic analysis of thermal inactivation of AMV RT was performed as described in Chapter 1.

Measurement of AMV RT activity for cDNA synthesis - The activity of AMV RT for cDNA synthesis was measured as described in Chapter 1. Briefly, the reaction (20 μl) was carried out in 25 mM Tris-HCl (pH 8.3), 50 mM KCl, 2.0 mM DTT, 0.1 mM dNTP, 0.5 μM R12 primer, 0.08 pg/μl standard RNA, 0.05 μg/μl *E. coli* RNA, and 10 nM AMV RT α subunit at a range of temperatures from 46 to 66ºC for 30 min and stopped by heating at 95ºC for 5 min. The PCR reaction was carried out, and then the amplified products were separated on 1.0% agarose gels.

Results

1) Production of AMV RT α subunit using insect cell expression system

Steady-state kinetic parameters of the αβ heterodimer and the α subunit - Starting with 100 ml of culture, about 20 μg of the purified α subunit was recovered. On SDS-PAGE under reducing conditions, the α subunit preparation thus obtained yielded a single band with a molecular mass of 63 kDa (Fig. 2B). The reverse transcriptase activities of the AMV RT αβ heterodimer and the α subunit were compared. Figure 3 shows the initial reaction rates incorporating dTTP into poly(rA)-p$(dT)_{15}$ at various dTTP concentrations (0-200 μM) with 10 nM RT at 37ºC. A saturated profile of the Michaelis-Menten kinetics was obtained, and the K_m and k_{cat} values were separately determined to be 137 ± 19 μM and 3.7 ± 0.3 s^{-1} respectively for the αβ heterodimer, and 107 ± 22 μM and 1.7 ± 0.2 s^{-1} respectively for the α subunit, indicating that their K_m

values were similar, and that the k_{cat} value of the α subunit was 50% of that of the αβ heterodimer.

Thermal stabilities of the αβ heterodimer and the α subunit - The thermal stabilities of the αβ heterodimer and the α subunit were compared. Figure 4A shows their irreversible thermal inactivation. RT at 100 nM in 10 mM potassium phosphate, 2.0 mM DTT, 0.2% Triton X-100, and 10% glycerol pH 7.6 was incubated in the absence and the presence of 28 μM T/P at various temperatures for the specified durations, followed by incubation on ice for 30-60 min. The remaining activity of the RT toward the incorporation of dTTP into T/P was determined at 37°C, as described above. Linear relationships between the natural logarithm of the remaining activity against incubation time were obtained at 48ºC (Fig. 4A) and all the other temperatures examined (44, 46, 50, and 52ºC) (data not shown), indicating that thermal inactivation can be regarded as a first-order reaction. Figure 4B shows an Arrhenius plot of the first-order rate constant, k_{obs}, of the thermal inactivation of the αβ heterodimer and the α subunit. A linear relationship held between the natural logarithm of k_{obs} and $1/T$. The temperatures required to reduce initial activity by 50% over a 10-min incubation (T_{50}) of the αβ heterodimer in the absence and in the presence of the T/P were estimated from the Arrhenius plot to be 48 and 51ºC respectively, while those of the α subunit were estimated to be 45-46ºC both in the absence and in the presence of the T/P. These results indicate that the thermal stability of the α subunit was lower than that of the αβ heterodimer, and that unlike the αβ heterodimer, the α subunit was not stabilized by the T/P.

2) Stabilization of AMV RT α subunit

Steady-state kinetic parameters of the wild-type α subunit and the variant V238R/L388R/D450A – We constructed the AMV RT α subunit variant V238R/L388R/D450A (which we termed "AM4"), and its characteristics was compared with that of the wild-type AMV RT α subunit (WT) to check whether the introduction of basic residues into the nucleic acid binding site of RT has an effect on the stabilization of AMV RT. WT and AM4 were expressed in insect cells and purified from the cells. Upon SDS-PAGE under reducing condition, both enzyme preparations yielded a single band with a molecular mass of 63 kDa, while MMLV RT, which was expressed in *E. coli* and purified from the cells (*12*), yielded a single band at 75 kDa (Fig. 5).

The kinetic parameters of the α subunits in the incorporation of dTTP into poly(rA)-p$(dT)_{15}$ (T/P) were examined. Figure 6 shows the initial reaction rates for 10 nM AMV RT α subunit at various T/P concentrations (0-25 μM) at 37ºC. A saturated profile of the Michaelis-Menten kinetics was obtained. The K_m and k_{cat} values were 18.8 ± 4.4 μM and 7.4 ± 0.9 s^{-1}, respectively, for WT, and 7.0 ± 0.9 μM and 7.7 ± 0.4 s^{-1}, respectively, for AM4, indicating that the K_m value of AM4 was 40% of that of WT, while their k_{cat} values were almost the same. This suggests that AM4 has higher affinity for T/P than WT.

Thermal stabilities of the wild-type α subunit and the variant V238R/L388R/D450A - The remaining reverse transcriptase activities of the AMV RT α

subunits were determined at 37ºC after thermal treatment (42-46ºC for WT and 46-50ºC for AM4) in the presence and the absence of T/P. Figure 7A shows the results with the thermal treatment at 46ºC (data not shown for the results with the treatment at other temperatures). The linear relationship between the natural logarithm of the remaining activity and the incubation time indicated that the inactivation followed pseudo-first-order kinetics. The relative activity of WT decreased to less than 10% at 25 min, while that of AM4 hardly decreased at 0-30 min, indicating that AM4 is more stable than WT.

Figure 7B shows an Arrhenius plot of k_{obs} of the thermal inactivation of the α subunits in the presence and the absence of T/P. The natural logarithm of k_{obs} and 1/T showed a linear relationship. The temperatures required to reduce initial activity by 50% over a 10-min incubation (T_{50}) were calculated by this plot. The T_{50} values without and with T/P of WT were 44.3 and 44.1ºC, respectively, and those of AM4 were 50.1 and 49.3ºC, respectively, indicating that AM4 is more stable than WT and that the α subunits were not stabilized by T/P. The activation energies (E_a) of thermal inactivation of the α subunits were calculated from the slope of this plot. The E_a values without and with T/P of WT were 194 ± 43 and 244 ± 40 kJ mol^{-1}, respectively, and those of AM4 were 240 ± 23 and 298 ± 0 kJ mol^{-1}, respectively, indicating that all E_a values were similar.

AMV RT α subunit-catalyzed cDNA synthesis - The activities of the α subunits for cDNA synthesis reaction were examined. cDNA synthesis reaction was carried out with WT and AM4 at 44-66ºC, followed by PCR of the cDNA synthesis reaction products. Figure 8 shows the results with agarose gel electrophoresis of the PCR products. The

highest temperatures at which the amplified product with the expected size of 601 bp was detected were 60ºC for WT and 64ºC for AM4, indicating that AM4 is more stable than WT in cDNA synthesis.

Discussion

Increase in RT stability by introducing positive charges by site-directed mutagenesis - In Chapter 1, the quadruple mutation of Glu286→Arg, Glu302→Lys, Leu435→Arg, and Asp524→Ala increased the highest temperature at which cDNA synthesis reaction occurred by 6ºC (from 54 to 60ºC), and decreased the K_m value for T/P to 40% of that without the mutation in the incorporation of dTTP into T/P (*39*). In this study of AMV RT α subunit, the triple mutation of Val238→Arg, Leu388→Arg, and Asp450→Ala, which corresponds to the quadruple mutation introduced into MMLV RT, increased the highest temperature at which cDNA synthesis reaction occurred by 4ºC (from 60 to 64ºC) (Fig. 8), and decreased the K_m value for T/P to 40% of that without the mutation in the incorporation of dTTP into T/P (Fig. 6). These results suggest that introduction of positive charges into the enzyme molecule at positions that have been implicated in the interaction with T/P by site-directed mutagenesis is effective to stabilize not only MMLV RT and AMV RT but also other RTs.

It is known that the mutations to abolish RNase H activity of RT increase its thermostability although its mechanism is not clarified (*14*, *24*). Except for such mutations, the stabilizing mutations so far reported in MMLV RT are Glu69→Lys, Glu302→Arg, Trp313→Phe, Leu435→Gly, and Asn454→Lys (*23*). Interestingly, these

mutations were developed by random mutagenesis, but the multiple variant E69K/E302R/W313F/L435G/N454K (M5) has lower K_m value for T/P than the wild-type MMLV RT (*23*). In HIV-1 RT, it was recently reported that the HIV-1 group O RT is more stable than HIV-1 group M (major-typed) RT and is as stable as MMLV RT (*40, 41*). The sequence homology between these two HIV-1 RTs is 21%, and the amino acid residues essential for the difference in stability have not been identified.

Another approach to develop thermostable reverse transcriptase is to generate RNA-dependent DNA polymerase activity in thermostable DNA-dependent DNA polymerase by a genetic engineering technique (*42*). Recently, double mutation of Leu329→Ala and Gln384→Ala in family A DNA polymerase from *Thermotoga petrophila* K4 generated RNA-dependent DNA polymerase activity although the magnitude of the RNA-dependent DNA polymerase activity was smaller than that of MMLV RT (*43*). In that study, the mutations were introduced at positions that have been implicated in the discrimination of DNA and RNA by steric interference with the 2'-hydroxyl group of ribose (*43*).

Effects of T/P on the stabilization of RT - The triple mutation of Val238→Arg, Leu388→Arg, and Asp450→Ala increased the T_{50} of AMV RT α subunit from 54 to 60ºC both in the presence and absence of T/P (Fig. 7). This means that T/P does not stabilize the wild-type AMV RT α subunit or its thermostable variant V238R/L388R/D450A (AM4). This is in contrast to that T/P stabilizes native AMV RT consisting of α and β subunits and native MMLV RT (*12, 14, 44*).

Integrase is the enzyme that is required for the integration of the viral DNA

synthesized in the host cell from the viral RNA genome into the host cell DNA genome. In AMV RT, the β subunit has the integrase domain, but the α subunit does not. Our results suggest that the intergrase domain is required for the stabilization of AMV RT by T/P. Without the integrase domain, introduced positive charges increase the affinity of AMV RT for T/P, but do not result in the stabilization by T/P. We hypothesize that unlike native AMV RT, introduced positive charges make AMV RT α subunit thermally resistant only by increasing intrinsic enzyme stability. This hypothesis should be explored by characterizing recombinant wild-type AMV RT heterodimer consisting of α and β subunits and its variant with the triple mutation of Val238→Arg, Leu388→Arg, and Asp450→Ala in the α and/or β subunits. It should be noted that the expression level of the β subunit in insect cells is markedly lower than that of the α subunit (data not shown), and thus optimization of preparation conditions need to be addressed.

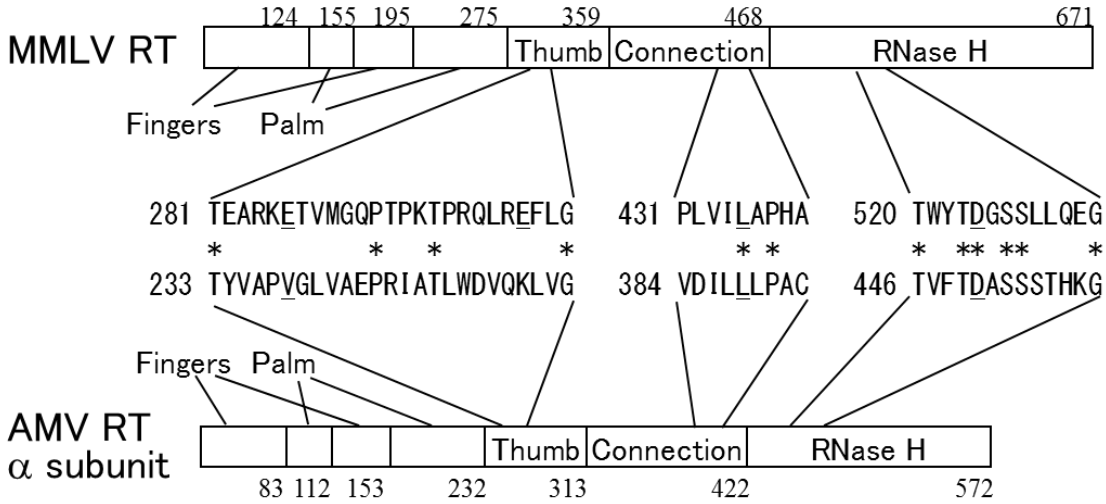

Fig. 1. Structure of MMLV RT and AMV RT α subunit. Amino acid numberings of MMLV RT (Thr24-Leu671) and AMV RT α subunit (Thr1-Tyr572) are according to GenBank accession codes J02255 and FJ041197, respectively. Asterisks show homologous amino acid residues. The amino acid residues to be mutated are underlined.

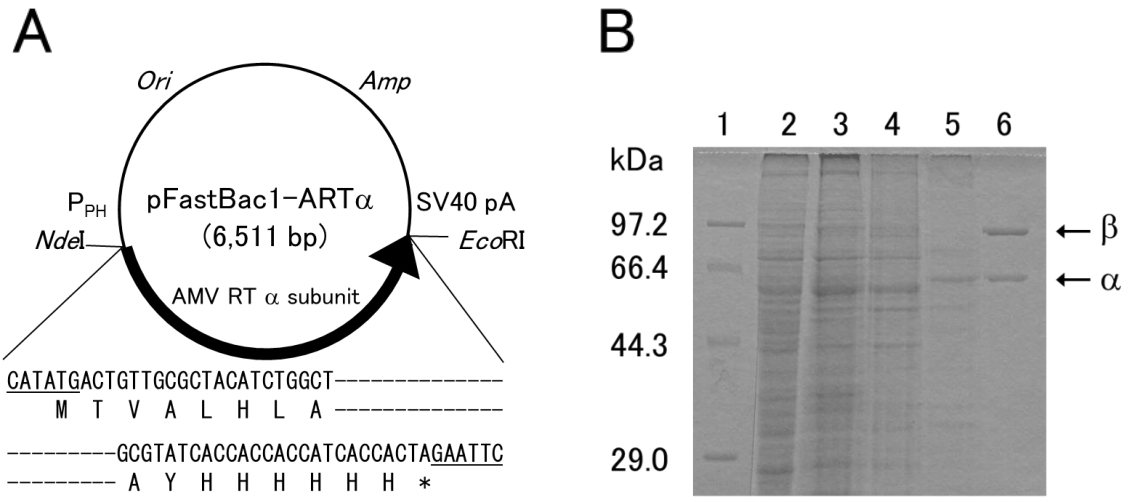

Fig. 2. Preparation of the recombinant AMV RT α subunit. (A) Structure of pFastBac1-ARTα. P_{PH} indicates polyhedron promoter. SV40 pA indicates SV40 polyadenylation signal. The *Nde*I and *Eco*RI sites are underlined. (B) Commassie Brilliant Blue-stained 10% SDS-polyacrylamide gel. Lane 1, molecular-mass marker; lane 2, the centrifuged supernatant after sonication of the Sf9 cells; lane 3, the centrifuged pellet after fractionation by ammonium sulfate of 40% saturation; lane 4, active fractions of anion-exchange column chromatography; lane 5, active fractions of Ni^{2+} affinity chromatography, which is the purified AMV RT α subunit; lane 6, the native AMV RT αβ heterodimer. The lower and upper arrows indicate the band, corresponding to the AMV RT α and β subunits respectively. The amino-acid and nucleotide sequences of AMV RT α were deposited with GenBank under accession no. FJ041197.

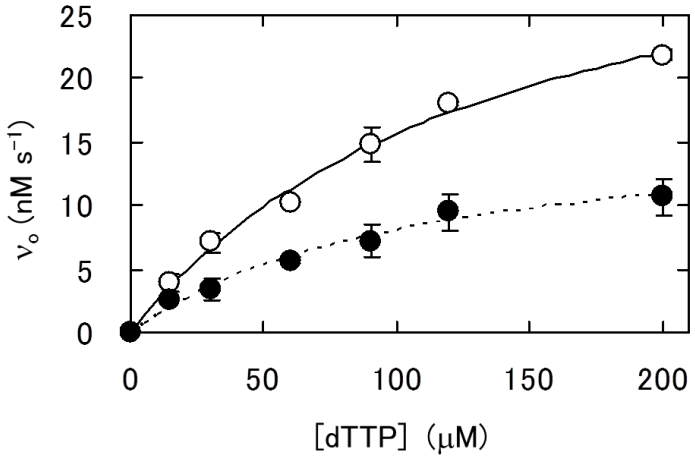

Fig. 3. Dependence on substrate concentration of the initial reaction rate of the RT-catalyzed reverse transcription reaction. The reaction was carried out with AMV RT αβ heterodimer (open circle) and α subunit (closed circle) at 10 nM at 37ºC. The concentration of poly(rA)-p$(dT)_{15}$ was 25 μM. Error bars indicate SD values for triplicate measurements. Solid and broken lines represent the best fit of the Michaelis-Menten equation by the non-linear least squares method.

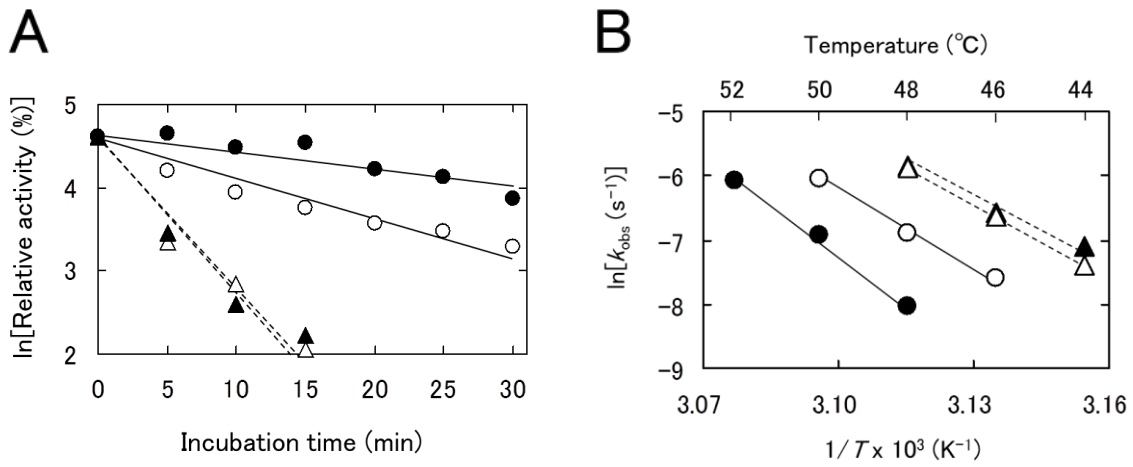

Fig. 4. Irreversible thermal inactivation of MMLV RT. The AMV RT αβ heterodimer and the α subunit, each at 100 nM, were incubated at 44-52ºC in the absence and the presence of poly(rA)-p$(dT)_{15}$ (T/P) (28 μM) for the indicated durations. The relative activity of RT in the reverse transcription reaction was defined as the ratio of the initial reaction rate with incubation for the indicated durations to that without incubation (19 nM s^{-1} for the αβ heterodimer and 8.4 nM s^{-1} for the α subunit). (A) Thermal inactivation at 48ºC. The first-order rate constant of the thermal inactivation of RT (k_{obs}) was estimated from the slope: αβ heterodimer without the T/P (open circle), 1.0×10^{-3} s^{-1}; αβ heterodimer with the T/P (closed circle), 3.2×10^{-4} s^{-1}; α subunit without the T/P (open triangle), 2.9×10^{-3} s^{-1}; α subunit with the T/P (closed triangle), 2.9×10^{-3} s^{-1}. One of the representative data of three separate experiments is shown. (B) Arrhenius plot of k_{obs} values. The activation energy of thermal inactivation of RT (E_a) was calculated from the slope: αβ heterodimer without the T/P (open circle), 327 ± 21 kJ mol^{-1}; αβ heterodimer with the T/P (closed circle), 424 ± 35 kJ mol^{-1}; α subunit without the T/P (open triangle), 332 ± 1 kJ mol^{-1}; α subunit with the T/P (closed triangle), 271 ± 29 kJ mol^{-1}.

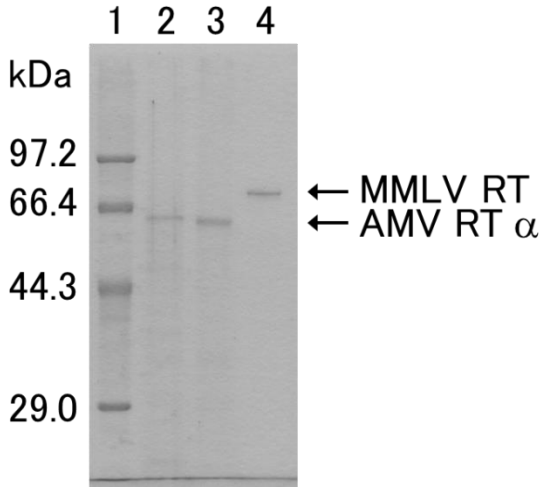

Fig. 5. SDS-PAGE under reducing conditions. Coomassie Brilliant Blue-stained 10% SDS-polyacrylamide gel is shown. Lane 1, molecular-mass marker; lane 2, wild-type AMV α subunit (WT); lane 3, AMV RT α subunit variant V238R/L388R/D450A (AM4); lane 4, wild-type MMLV RT.

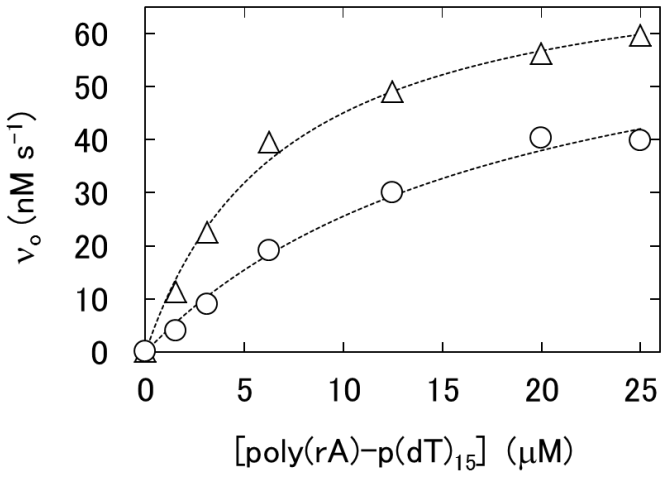

Fig. 6. Dependence on substrate concentration of the initial reaction rate of AMV RT α subunit-catalyzed incorporation of dTTP into poly(rA)-p(dT)$_{15}$ at 37°C. The initial concentrations of AMV RT α subunit and dTTP were 10 nM and 200 μM, respectively. Solid lines represent the best fit of the Michaelis-Menten equation with the non-linear least squares method. Symbols for the enzymes: WT, open circle; AM4, open triangle. The average of triplicate determination is shown.

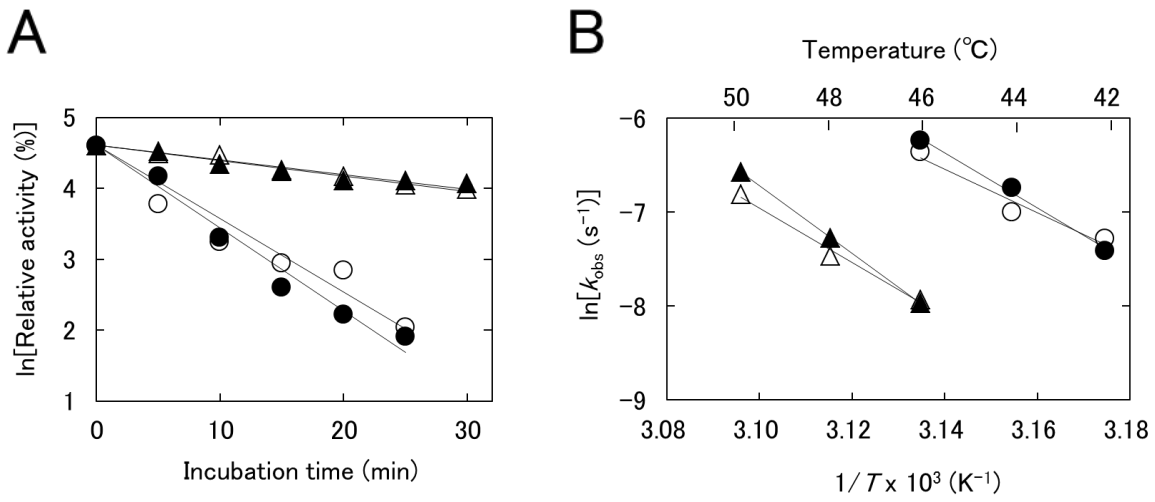

Fig. 7. Irreversible thermal inactivation of AMV RT α subunit. AMV RT α subunit at 30 nM was incubated at 42-50°C in the presence or absence of poly(rA)-p(dT)$_{15}$ (T/P) (28 μM) for the indicated durations. Then, the reverse transcription reaction was carried out at 37°C. The relative activity of AMV RT α subunit was defined as the ratio of the initial reaction rate with incubation for the indicated durations to that without incubation [14.8 nM s^{-1} for WT (3 nM) without T/P, 16.2 nM s^{-1} for WT (3 nM) with T/P, 18.9 nM s^{-1} for AM4 (3 nM) without T/P, 19.3 nM s^{-1} for AM4 (3 nM) with T/P]. (A) Irreversible thermal inactivation at 46ºC. The first-order rate constant of the thermal inactivation (k_{obs}) of RT was estimated from the slope: WT without T/P (open circle), 1.9×10^{-3} s^{-1}; WT with T/P (closed circle), 1.7×10^{-3} s^{-1}; AM4 without T/P (open triangle), 3.6×10^{-4} s^{-1}; AM4 with T/P (closed triangle), 3.5×10^{-4} s^{-1}. (B) Arrhenius plot of k_{obs} values. The activation energy of thermal inactivation (E_a) of RT with or without T/P was calculated from the slope: WT without T/P (open circle), 194 ± 43 kJ mol^{-1}; WT with T/P (closed circle), 244 ± 40 kJ mol^{-1}; AM4 without T/P (open triangle), 240 ± 23 kJ mol^{-1}; AM4 with T/P (closed triangle), 298 ± 0 kJ mol^{-1}.

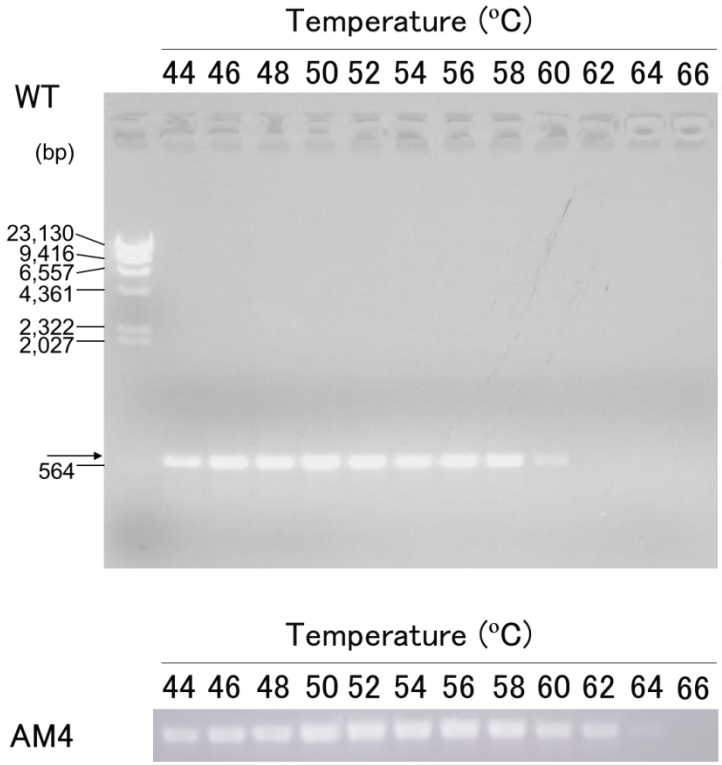

Fig. 8. Dependence on reaction temperature of cDNA synthesis by AMV RT α subunit. cDNA synthesis was carried out with 1.6 pg *cesA* RNA, 0.2 μM RV-R12 primer, and 10 nM AMV RT α subunit at 44-66°C. PCR was carried out with a primer combination of RV and F5. Amplified products were applied to 1.0% agarose gel followed by staining with ethidium bromide (1 μg/ml). The arrow indicates the expected size (601 bp) of the amplified products.

Chapter 3

Exploration of thermostabilization mechanism of reverse transcriptase

Introduction

We have produced the thermostable RTs by introducing basic residues in the nucleic acid binding cleft of the RT in Chapters 1 and 2. In those studies, we hypothesized that the introduction of positive charges increases the thermostability of MMLV RT by improving its ability to bind the T/P that is negatively charged. However, the stabilization mechanism of MMLV RT is still unknown. In Chapter 3, we show evidence that reveals that mutations, E286→R, E302→K, and L435→R, responsible for the higher thermal stability of the RT, do not affect T/P binding affinity, but abolish the RNase H activity of the polymerase.

Materials and methods

Expression and purification of recombinant MMLV RT - Recombinant MMLV RT was prepared as described previously (*24*). *Escherichia coli* strain BL21(DE3) was transformed with the pET-22b(+) plasmid (Merck Bioscience, Tokyo, Japan) harboring the nucleotides sequence encoding the MMLV RT with a C-terminal $(His)_6$-tag. *E. coli* cells were harvested from a 2-liter culture, and resuspended in 20 ml of 20 mM

potassium phosphate (pH 7.2) buffer, containing 2 mM dithiothreitol (DTT) and 10% (v/v) glycerol (buffer A). After adding 1 mM phenylmethylsulfonyl fluoride (PMSF) to buffer A, cells were sonicated. After centrifugation at 20,000 x g for 40 min, the supernatant was collected and applied to a column [25 mm (inner diameter) x 120 mm] packed with Toyopearl DEAE-650 M gel (Tosoh, Tokyo, Japan), previously equilibrated with buffer A. The column was washed with 80 ml of buffer A containing 120 mM NaCl and eluted with buffer A containing 300 mM NaCl, to which saturated $(NH_4)_2SO_4$ was added to a final 40% saturation. After centrifugation at 20,000 x g for 30 min, the pellet was collected and dissolved in 10 ml of buffer A containing 500 mM NaCl. After centrifugation at 20,000 x g for 5 min, the supernatant was applied to the column packed with a Ni^{2+}-Sepharose^{TM} (HisTrap HP 1 ml, GE Healthcare, Buckinghamshire, UK), previously equilibrated with buffer A. The column was washed with 50 ml of 50 mM Tris-HCl (pH 8.3) buffer, containing 200 mM KCl, 2 mM DTT, 10% glycerol, and 50 mM imidazole, and the RT was eluted with 3 ml of 50 mM Tris-HCl (pH 8.3) buffer, containing 200 mM KCl, 2 mM DTT, 10% glycerol, and 500 mM imidazole. The eluate was then applied to the column packed with a Sephadex G-25 (PD-10, GE Healthcare), previously equilibrated with 50 mM Tris-HCl (pH 8.3), containing 200 mM KCl and 50% glycerol (buffer B). The column was washed and eluted with the same buffer. This sequential chromatography procedures consisting of the Ni^{2+}-Sepharose^{TM} column and the Sephadex G-25 column were repeated two more times. The eluate at the final step was further purified by chromatography on the Sephadex G-25 column. Purified MMLV RT was stored at -80ºC before use. MMLV RT concentration was determined using the Protein Assay CBB Solution (Nacalai Tesque, Kyoto, Japan) using bovine serum albumin as standard.

Irreversible thermal inactivation of MMLV RT - MMLV RT (100 nM) in 10 mM potassium phosphate (pH 7.6) buffer, containing 2 mM DTT, 0.2% Triton X-100, and 10% glycerol was incubated in the presence and absence of 28 μM poly(rA)-p$(dT)_{15}$ at 50°C for 10 min followed by incubation on ice for 30 min. The residual DNA polymerase activity of MMLV RT was measured as described previously (*39*). Briefly, the reaction was carried out in 25 mM Tris-HCl (pH 8.3) buffer, containing 50 mM KCl, 2 mM DTT, 5 mM $MgCl_2$, 25 μM poly(rA)-p$(dT)_{15}$ (this concentration is expressed as that of p$(dT)_{15}$), 0.2 mM [^{3}H]dTTP, and 10 nM MMLV RT at 37ºC. Aliquots of 20 μl were collected at different times and immediately spotted onto glass microfiber filters GF/C of 2.5 cm (Whatman, Middlesex, UK). Unincorporated [^{3}H]dTTP was removed by three washes with chilled 5% (w/v) trichloroacetic acid for 10 min each followed by one wash with chilled 95% ethanol. The amounts of [^{3}H]dTTP incorporated were determined by scintillation counting in 2.5 ml of Ecoscint H solution (National Diagnostics, Atlanta, GA) using a LSC-5100 apparatus (Aloka, Mitaka, Japan), and the initial reaction rate was determined.

Determination of dissociation constants (K_d) of RT-T/P complex - The 31T(DNA) or the 31T (RNA) and the 21P-C(DNA) labelled with [γ-^{32}P]ATP (PerkinElmer, Boston, MA) at its 5'-terminus were annealed to generate T/Ps 31T(DNA)/[^{32}P]21P-C(DNA) and 31T(RNA)/[^{32}P]21P-C(DNA). MMLV RTs (12 nM) were pre-incubated with various concentrations of either of the two duplexes (2-40 nM) at 37ºC for 10 min in 20 μl of 50 mM Tris-HCl (pH 8.0) buffer, containing 50 mM KCl. Reactions were initiated by adding 20 μl of 50 mM Tris-HCl (pH 8.0) buffer, containing 20 mM dTTP, 50 mM

KCl, 30 mM $MgCl_2$, and 20 μM 31T(DNA)/21P-C(DNA). The 31T(DNA)/21P-C(DNA) at high concentration (20 μM) binds unbound RT as well as RT that dissociates from DNA/DNA or RNA/DNA duplexes, preventing further RT binding to labelled T/Ps. Aliquots of 4 μl were removed at 15, 30, and 45 s, and immediately quenched with 4 μl of sample-loading buffer (10 mM EDTA, 90% (v/v) formamide, 3 mg/ml xylene cyanol FF, 3 mg/ml bromophenol blue, and 50 μM 31T(DNA)/21P-C(DNA)). The reaction products were analyzed by denaturing 20% polyacrylamide gel electrophoresis and quantified with a BAS-2500 scanner (Fujifilm, Tokyo, Japan) using the program Multi Gauge version 2.2 (Fujifilm). For each reaction, the percentage of elongated primer was plotted against the incubation times and the data were fit to a linear equation. As the concentration of template-primer is well above the dissociation constant of MMLV RT, K_d, under this assay conditions, the RT-T/P concentration, [RT-T/P], in the preincubated mixture was calculated from the *y*-intercept that represents the amount of RT bound to template-primer at time zero. The K_d values were determined by fitting the data thus obtained to Eq. 1.

$$[\text{RT-T/P}] = 0.5\times(K_d+[\text{RT}]_o+[\text{T/P}]_o) - 0.5\times\{(K_d+[\text{RT}]_o+[\text{T/P}]_o)^2 - 4[\text{RT}]_o[\text{T/P}]_o\}^{0.5} \quad (1)$$

where K_d is the dissociation constant of MMLV RT with T/P, and $[RT]_o$ and $[T/P]_o$ are the initial RT and T/P concentration, respectively, in the preincubated mixture. The relative RT-T/P concentration, defined as the ratio of the respective RT-T/P concentration to the maximum values obtained, was plotted as a function of the initial T/P concentration.

Extension of primers in the absence of one dNTP - The DNA polymerase activity of MMLV RT in the absence of one dNTP was determined using a method previously described (*45*). Briefly, the reaction (40 µl) was carried out at 37ºC in 50 mM Tris-HCl (pH 8.0) buffer, containing 50 mM KCl, 15 mM $MgCl_2$, 150 nM MMLV RT, 20 nM D2-47(DNA)/[^{32}P]PG5-25(DNA), and 250 µM each dNTP. The reaction was stopped after a two-hour incubation, and the reaction products were analyzed as described above (section "*Determination of dissociation constants (K_d) of RT-T/P complex*").

RNase H activity assay - The RNase H activity of MMLV RT was determined as described previously (*40*). Briefly, four RNA/DNA duplexes were prepared. The reaction (40 µl) was carried out in 50 mM Tris-HCl (pH 8.0) buffer, containing 50 mM KCl, 15 mM $MgCl_2$, 150 nM MMLV RT, and 20 nM [^{32}P]31T(RNA)/21P-C(DNA), [^{32}P]D2-47(RNA)/PG5-25(DNA), [^{32}P]D2-25(RNA)/PG5-25(DNA), or [^{32}P]31T(RNA)/15P(DNA) at 37ºC for 0-40 min. Then aliquots were removed at different times (0.25, 0.5, 2, 4, 20, and 40 min), and reaction products were analyzed as described above (section "*Determination of dissociation constants (K_d) of RT-T/P complex*").

Results

Preparation and characterization of MMLV RT - We previously generated four thermostable MMLV RT variants by introducing single amino acid substitutions (E286R, E302K, L435R, and D524A) as well as one quadruple variant

(E286R/E302K/L435R/D524A, designated as MM4) (*39*). Wild-type enzyme (WT) and all mutant RTs were expressed in *E. coli* and purified to homogeneity. RTs were judged to be pure by SDS-PAGE, and the M_r values obtained were around 75,000 (Fig. 1A).

DNA polymerase activities of all enzymes were determined at 37ºC after incubation at 50ºC for 10 min in the presence and absence of T/P (Fig. 1B). Each enzyme exhibited higher relative activity in the presence of T/P than in its absence, and all variants exhibited higher relative activities than WT both in the presence and the absence of T/P. These results are in agreement with those published in our previous report (*39*).

We measured UV, CD, and fluorescence spectra of the purified enzymes. All enzymes exhibited similar UV spectra with maximum absorbance at 275 nm (Fig. 2A). On CD spectroscopy, all RTs exhibited negative ellipticities at around 202–250 nm with minimum values around 208 and 222 nm (Fig. 2B). At excitation wavelength of 280 and 295 nm, all RTs exhibited emission fluorescence spectra with maximum intensities at 338 nm (Fig. 2C and D). No appreciable changes were observed in each spectra between WT and variants.

Effect of stabilizing mutations on the affinities of MMLV RT for T/P - In order to test whether individual mutations such as E286→R, E302→K, and L435→R would affect T/P binding affinity, we determined the dissociation constants (K_d) of RT-T/P complexes. RTs were pre-incubated with various concentrations of radiolabelled T/P to form an RT-T/P complex. The reaction was initiated by adding dTTP, Mg^{2+}, and an excess of unlabelled T/P, and the products were analyzed. Figure 3 shows the relative concentraton of the RT-T/P complex *versus* the total T/P concentration in the

preincubated mixture. Saturation curves were obtained for DNA/DNA (Fig. 3A) and RNA/DNA (Fig. 3B) duplexes. The K_d values obtained with the DNA/DNA duplex and RTs WT, E286R, E302K, L435R, D524A, and MM4 were 2.9±0.3, 3.5±0.6, 6.5±1.2, 5.4±0.5, 3.3±0.4, and 2.9±0.3 nM, respectively, and the values obtained with the RNA/DNA duplex were 2.0±0.3, 1.7±0.2, 2.9±0.3, 2.7±0.4, 2.6±0.2, and 1.2±0.2 nM, respectively. These data indicate that WT and mutant RTs have similar binding affinities for T/P. The results also show that the binding affinities of MMLV RTs for the RNA/DNA duplex (K_d values of 1.2–2.9 nM) are slightly higher than for the DNA/DNA duplex (2.9–6.5 nM).

Effect of the stabilizing mutations on the fidelities of MMLV RT - The effects of stabilizing mutations on the fidelity of MMLV RT were determined by measuring primer extension in the absence of one dNTP (Fig. 4). In the presence of all four dNTPs, fully-extended products of 47-nucleotides (nt) were obtained with all enzymes. In the absence of dGTP, the same result was obtained, compatible with the sequence of D2-47/PG5-25 in which dGTP is not required for faithful extension. When dATP was absent, in WT, E286R, L435R, and D524A, the intensities of the bands corresponding to 42- and 43-nt products were similar, while in reactions carried out with mutants E302K and MM4, the intensity of the 42-nt band was stronger than the intensity of the 43-nt band. This result is consistent with a lower misincorporation of A at position 43, by mutant E302K, suggesting that this mutation increases the fidelity of MMLV RT, while E286→R, L435→R, and D524→A do not.

Effect of the stabilizing mutations on the RNase H activities of MMLV RT - It is

known that the loss of RNase H activity caused by the mutation of the catalytic residue, Asp524, increases the stability of the RNA in reverse transcription reactions and improves the efficiency of the DNA polymerase activity (*14*). In order to determine whether the three stabilizing mutations affect the RNase H activity, we measured the RNase H activities of WT and mutant enzymes with the RNA/DNA hybrid, [^{32}P]31T(RNA)/21P-C(DNA), consisting of 31-nt RNA and 21-nt DNA as the substrate (Fig. 5A). In reactions carried out with WT RT, evidence of cleavage was demonstrated by the presence of RNA bands of 28-nt or smaller, indicating that the RNA strand of the hybrid was first cleaved at the position of 18-bp upstream of the primer 3'-teriminus. As expected, in D524A and MM4 of which the catalytic residue for RNase H activity, Asp524, is mutated to Ala, RNA remained undegraded. Unexpectedly, the mutants E286R, E302K, and L435R did not show RNase H activity, and RNA templates remained uncleaved after 40-min incubation at 37ºC (Fig. 5A).

In reactions carried out with HIV-1 RT, the RNA strand of an RNA/DNA hybrid is cleaved at the position of 16-bp upstream of the primer 3'-terminus (*46*), and that such T/P binds HIV-1 RT at its both DNA polymerase and RNase H active sites (*47*), suggesting that the RNase H activity of MMLV RT varies depending on RNA/DNA hybrid species. To address this possibility, we used three additional RNA/DNA hybrids ([^{32}P]D2-47(RNA)/PG5-25(DNA) (Fig. 5B), [^{32}P]D2-25(RNA)/PG5-25(DNA) (Fig. 5C), and [^{32}P]31T(RNA)/15P(DNA)) (Fig. 5D). Each T/P was designed to bind to both the DNA polymerase and RNase H active sites simultaneously, to bind only the RNase H active site due to the lack of primer 3'-terminus, and to bind either of the two active sites but not both simultaneously due to the usage of a shorter primer, respectively. With all RNA/DNA hybrid species, RNAs remained uncleaved in reactions catalyzed by all

mutant RTs. This clearly indicates that mutations E286→R, E302→K, and L435→R abrogate the RNase H activity.

Discussion

Mechanism of the loss of RNase H activity by the stabilizing mutations - In this study, we demonstrate that the three stabilizing mutations (E286→R, E302→K, and L435→R) eliminate the RNase H activity of MMLV RT. The crystal structure of the full-length enzyme has not been determined. Crystal structures of the polymerase domains of MMLV RT and the closely related xenotropic murine leukemia virus-related virus (XMRV) RT have been partially determined (*6, 48*). These structures reveal the common fold consisting of fingers, palm, thumb, and connection subdomains found in HIV-1 RT. On the other hand, the structures of the isolated RNase H domains of the MMLV RT and XMRV RT have also been determined (*7, 49*). Molecular models of MMLV RT suggest that the RNase H domain of MMLV RT is positioned far from the fingers/palm/thumb subdomain, like in the structure of the p66 subunit of HIV-1 RT (*6, 8*). Based on those models, it has been suggested that the RNase H domain alters the trajectory of the T/P, affecting the DNA polymerase activity (*6, 8*). Moreover, it has been reported that the DNA polymerase activity of a MMLV RT variant lacking the RNase H domain was considerably reduced (*50*).

Amino acid sequence identity between MMLV and XMRV RTs is around 95% (*51*). The structure of the polymerase domain of XMRV RT bound to an RNA/DNA complex (*48*) reveals that Glu302 interacts with the T/P, but Glu286 and Leu435 are away from

the nucleic acid binding cleft and long-distance effects appear to be responsible for the lack of RNase H activity of the corresponding mutants (Fig. 6).

In addition, the results of fidelity assays show that mutations that increase the thermal stability of the MMLV RT have a relatively minor effect on the accuracy of the polymerase. Among the studied mutations, only E302→K produced a very modest improvement in the fidelity of the enzyme, detected only at selected sites in primer extension assays carried out in the absence of one nucleotide (Fig. 4).

In our study, all variants lacked RNase H activity, as demonstrated using four different RNA/DNA substrates. Two of them were designed with a template overhang to cover the DNA polymerase and the RNase H active sites simultaneously (Fig. 5A and B), a third substrate lacks the overhang and would bind only to the RNase H active site (Fig. 5C), while the fourth one is expected to bind any of the two active sites, but not both simultaneously, due to the relatively short distance between the 3´ end of the DNA primer and the putative RNase H cleavage site (Fig. 5D).

Taking into account the structures of those substrates, we suggest that the three stabilizing mutations would alter the trajectory of the T/P and prevent its proper binding at the RNase H active site, leading to the loss of the RNase H activity. This is in contrast to the case with the mutation of the catalytic residue for the RNase H activity, Asp524. In this case, the RNase H active site cannot bind Mg^{2+}, leading to the loss of RNase H activity. In addition, it should be mentioned that the rate of the degradation reaction observed with the WT RT and the substrate [^{32}P]D2-25(RNA)/PG5-25(DNA) (Fig. 5C) is similar to rates calculated from assays shown in Figs. 5A and B, suggesting the possibility that the substrate used in Fig. 5C binds both the DNA polymerase and RNase H active sites simultaneously.

Mechanism of the thermostabilization by the stabilizing mutations - In this study, we also suggest that the three stabilizing mutations increase the thermostability of MMLV RT not by increasing its affinity for the T/P but by abolishing its RNase H activity. Although it has been reported that the thermostabilities of MMLV, AMV, and HIV-1 RTs are improved by the loss of the RNase H activity through the elimination of the RNase H activity (*14*, *24*, *52-54*), the mechanism is unknown. Goedken and Marqusee reported that in the CD analysis of the reversible unfolding of the isolated RNase H domain of MMLV RT (Pro515-Leu671), the midpoint denaturation temperature of D524N was higher by 10ºC than that of the WT RT, suggesting that the substitution of Asp524 eliminates the RT's RNase H activity, leading to an increase in the enzyme's intrinsic thermostability as a result of a structural change (*55*). In the cases of E286R, E302K, and L435R, it was first thought that the observed higher thermostability was due to the increase in the T/P binding affinity (*39*). However, this has been challenged by our data showing that WT and mutant RTs exhibit similar K_d values (Fig. 3). As in the case of D524→A, amino acids changes E286→R, E302→K, and L435→R increase the RT's intrinsic thermal stability. Those mutations outside the RNase H catalytic site abolish the RNase H activity of the enzyme but do not affect its affinity for T/P.

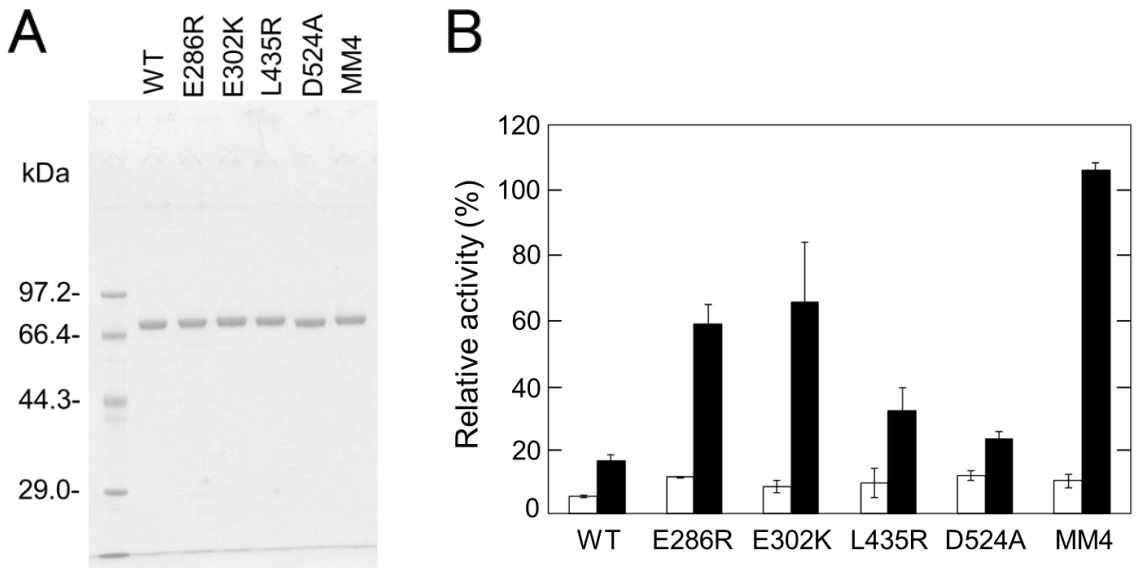

Fig. 1. Purification and characterization of MMLV RT. (A) SDS-PAGE under reducing conditions. Enzyme (1.2 μg) was applied to each lane. Coomassie Brilliant Blue-stained 10% SDS-polyacrylamide gels is shown. (B) Irreversible thermal inactivation of MMLV RT. Enzyme was incubated at 50ºC for 10 min in the presence (black bar) and the absence (whilte bar) of poly(rA)-p$(dT)_{15}$. Then, the dTTP incorporation reaction using poly(rA)-p$(dT)_{15}$ as T/P was carried out at 37ºC. The relative activity was defined as the ratio of the initial reaction rate with heat treatment to that without it. Represented values were obtained from at least three independent experiments.

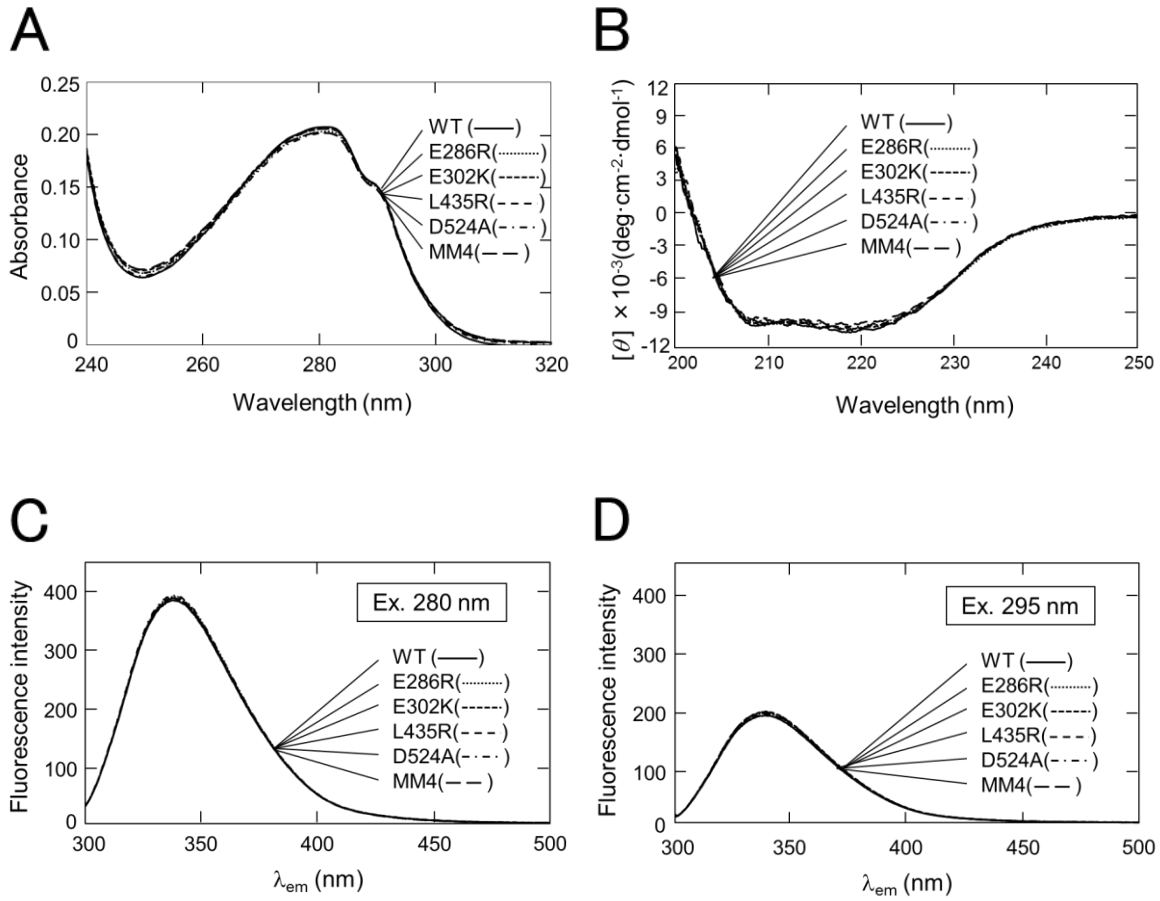

Fig. 2. UV, CD, and fluorescence spectra of MMLV RT. (A) UV spectra. (B) CD spectra. (C, D) Fluorescence spectra. Spectra were obtained in 50 mM Tris-HCl (pH 8.3) buffer, containing 200 mM KCl and 50% (v/v) glycerol at 25ºC with protein concentration of 0.15 mg/ml (A, B) or 0.075 mg/ml (C, D).

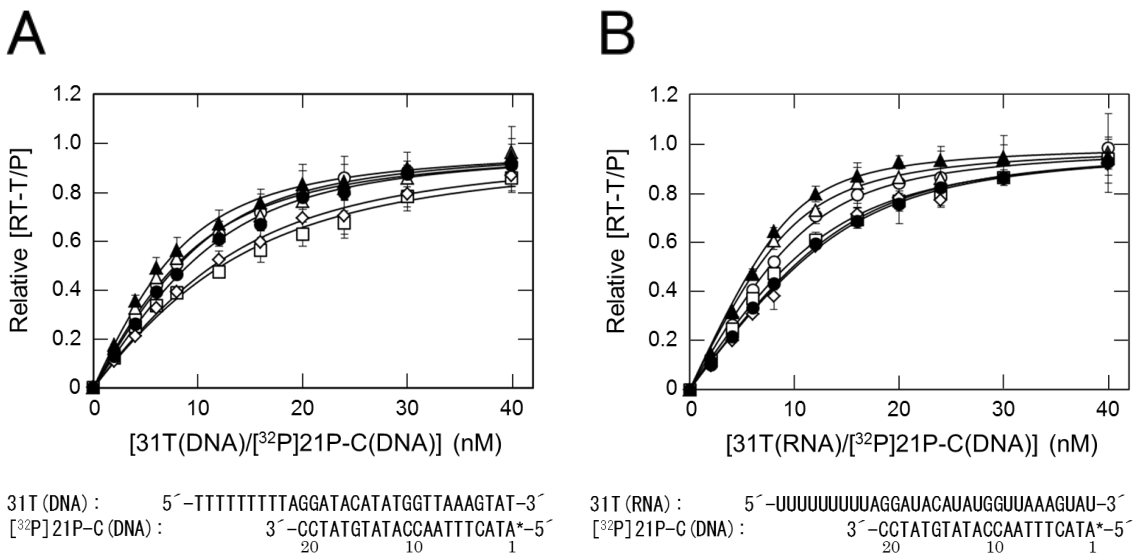

Fig. 3. Dissocation equilibrium of WT and mutant RTs with DNA/DNA and RNA/DNA complexes. WT and mutant RTs were preincubated with various concentrations of 31T(DNA)/[^{32}P]21P-C(DNA) (A) or 31T(RNA)/[^{32}P]21P-C(DNA) (B) at 37ºC for 10 min. DNA polymerization reactons were intiated by adding dTTP and unlabelled 31T(DNA)/21P-C(DNA). The initial concentrations of RT, dTTP, and unlabelled 31T(DNA)/21P-C(DNA) in the reaction were 6 nM, 10 mM, and 40 μM, respectively. The solid line is the best fit of the data to Eq. 1. The asterisk indicates the labelled nucleotide with [γ-^{32}P]ATP. Symbols: WT, open circle; E286R, open triangle; E302K, open square; L435R, open diamond; D524A, closed circle; and MM4, closed triangle.

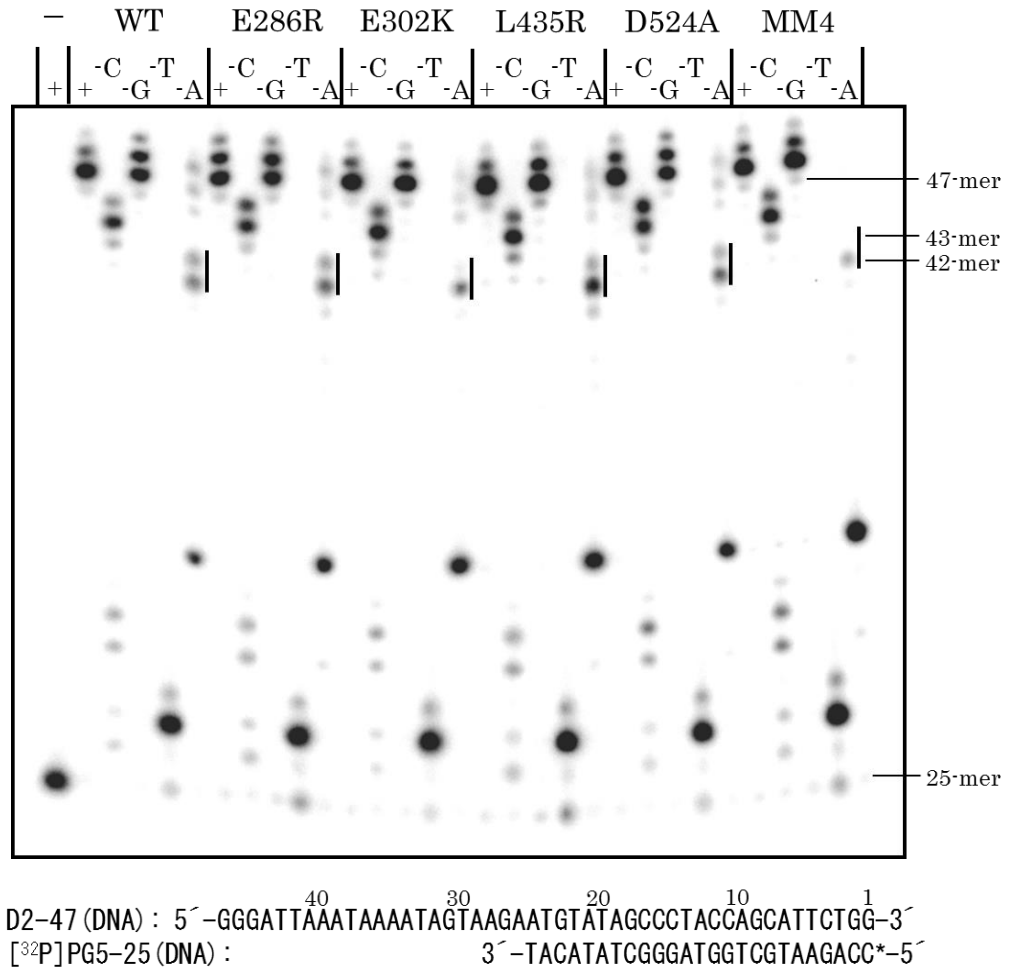

Fig. 4. Primer extension in the absence of one nucleotide. Reactions were carried out at 37ºC for 2 h with 150 nM MMLV RT, 20 nM D2-47(DNA)/[^{32}P]PG5-25(DNA), and 250 μM each dNTP. Lanes marked with + indicate that all four nucleotides were included in the dNTP mix. The lanes marked with -C, -G, -T, and -A indicate that three nucleotides except dCTP, dGTP, dTTP, or dATP, respectively. Specific bands corresponding to products of 42- and 43-nucleotides are indicated.

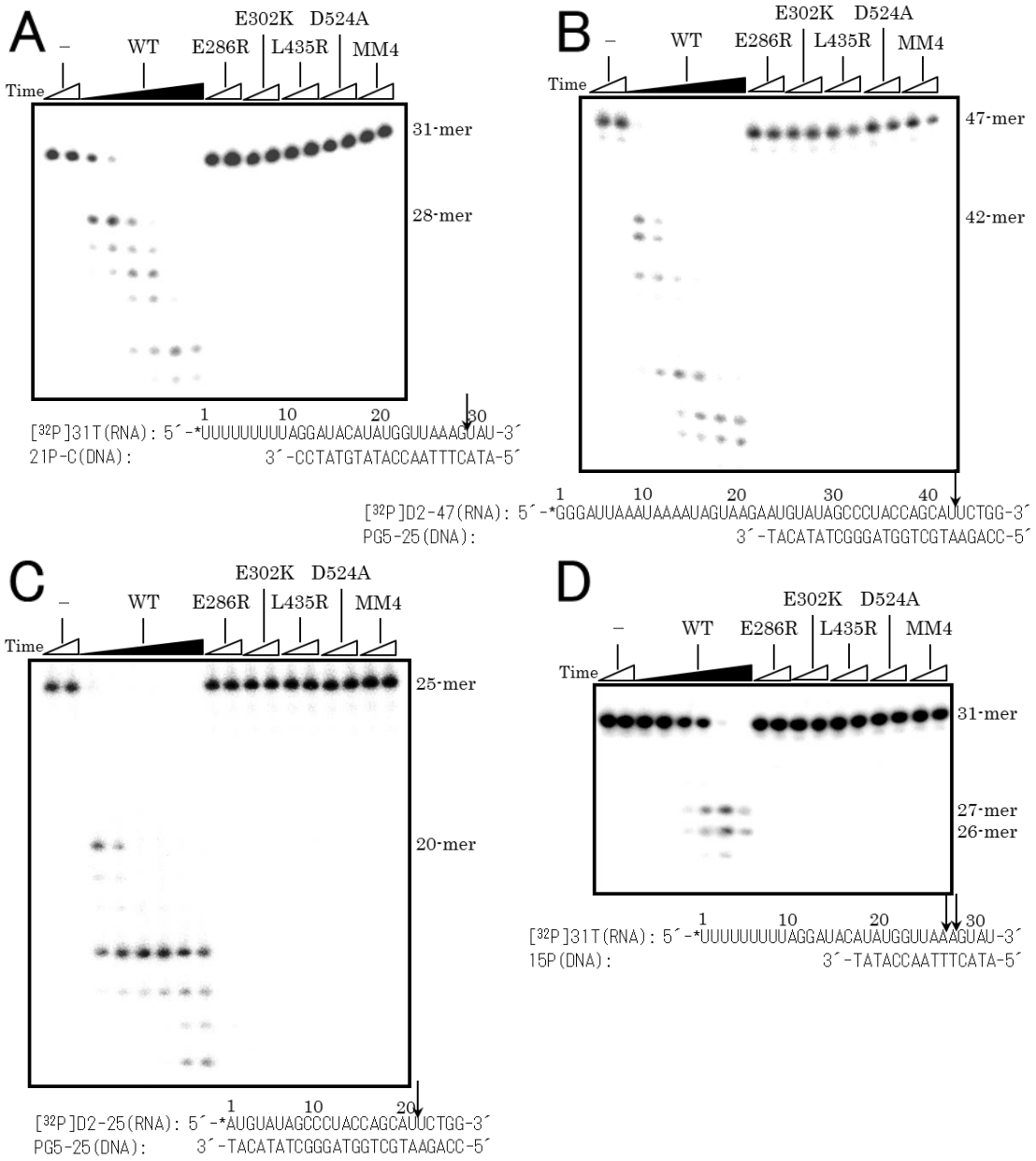

Fig. 5. RNase H activity. Reactions were carried out at 37ºC for 0-40 min in the presence of 20 nM labelled T/P and 0 or 150 nM RT. The arrows indicate the cleavage sites. Labelled T/P: A, [^{32}P]31T(RNA)/21P-C(DNA); B, [^{32}P]D2-47(RNA)/PG5-25(DNA); C, [^{32}P]D2-25(RNA)/PG5-25(DNA); D, [^{32}P]31T(RNA)/15P(DNA). The asterisk indicates the position of the ^{32}P label. Time points were 0.25, 0.50, 2.0, 4.0, 20, and 40 min for WT and 0.25 and 40 min for mutant RTs.

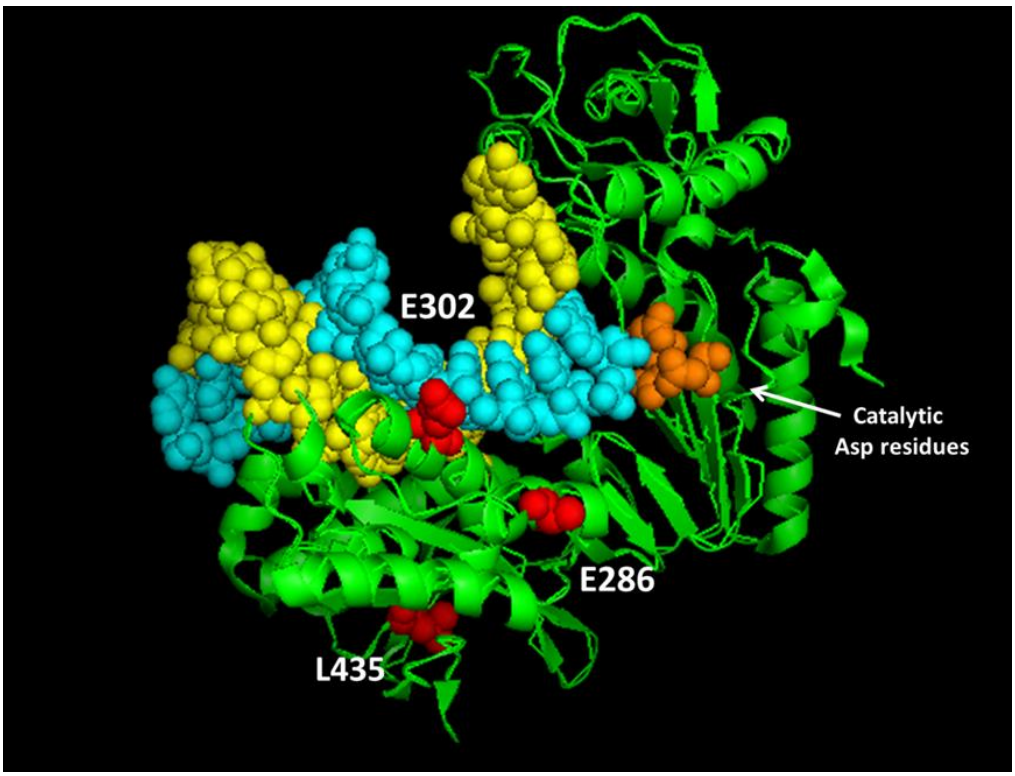

Fig. 6. Location of relevant residues in the crystal structure of the polymerase domain of XMRV RT. The RT backbone is represented with a green cartoon, the RNA/DNA template-primer is shown with spheres (yellow and cyan). Catalytic aspartic acid residues (positions 150, 225, and 226) are shown with orange spheres. Residues equivalent to those replaced in the MMLV RT are indicated in red (i.e. Glu286, Glu302, and Leu435). Coordinates were taken from Protein Data Bank file 4HKQ and the structure was drawn using the PyMol molecular software (http://www.pymol.org).

Summary

Chapter 1

We hypothesized that MMLV RT will increase with increases in its ability to bind with T/P. To test this hypothesis, we introduced positive charges into MMLV RT by site-directed mutagenesis at positions that have been implicated in the interaction with T/P. Thirty-six variants were constructed in which one of twelve residues (Glu69, Gln84, Asp108, Asp114, Glu117, Glu123, Asp124, Glu286, Glu302, Trp313, Leu435, and Asn454) was replaced with Lys, Arg, or Ala, and these were expressed in *E. coli*. In about half of these 36 variants, thermal inactivation at 50ºC was reduced in the presence of the T/P, which suggested that this strategy was effective at stabilizing MMLV RT. We next combined three of the 36 mutations, Glu286→Ala, Glu302→Lys, and Leu435→Arg, and the mutation, Asp524→Ala, which is known to abolish the RNase H activity and increase the stability. Temperatures of 54 and 56ºC reduced the initial reverse transcriptase activity by 50% over a 10-min incubation in the triple variant E286R/E302K/L435R (MM3) and quadruple variant E286R/E302K/L435R/D524A (MM4), respectively. These temperatures were higher than that observed for WT (45ºC). The highest temperatures at which MM3 and MM4 exhibited cDNA synthesis activity were 60ºC, which was again higher than for WT (54ºC). Single variants of Moloney murine leukemia virus reverse transcriptase, V433R and V433K, in which a surface hydrophobic residue, Val433, was mutated, retained 55% of initial reverse transcriptase

activity, while the wild-type enzyme retained 17% after thermal incubation at 48°C for 10 min. After thermal incubation at 50ºC for 10 min, multiple variants D108R/E286R/V433R (MM7) and D108R/E286R/V433R/D524A (MM8), in which Val433→Arg was combined with stabilizing mutations we have identified, Asp108→Arg and Glu286→Arg, and RNase H activity-eliminating mutation Asp524→Ala retained 70% of initial activity, exhibiting higher stability than V433R or V433K. Thus, highly stable MMLV RT variants MM3, MM4, MM7, and MM8 were generated by these mutation strategies.

Chapter 2

We established a new method for the production of AMV RT α subunit by using insect cells, and introduced into AMV RT α subunit the corresponding mutations, V238→R, L388→R, D450→A, which were comparable to the stabilizing mutations of MMLV RT (Chapter 1). The recombinant wild-type AMV RT α subunit (WT) was expressed in insect cells and purified. It exhibited lower thermal stability than the native AMV RT αβ heterodimer. Unlike the αβ heterodimer, WT was not stabilized by template-primer. These results suggest that interaction between the α and β subunits is important for AMV RT stability. The temperatures reducing initial activity by 50% in 10-min incubation of the variant V238R/L388R/D450A (AM4) with or without template primer (T/P), poly(rA)-p$(dT)_{15}$, were 50ºC, higher than for the wild-type AMV RT α subunit WT (44ºC). The highest temperature at which AM4 exhibited cDNA synthesis

activity was 64ºC, higher than for WT (60ºC). These results indicate that highly stable AMV RT α subunit was generated by the same mutation strategy as applied to MMLV RT, that positive charges are introduced into RT at positions that have been implicated to interact with T/P by site-directed mutagenesis.

Chapter 3

In Chapter 1, we used site-directed mutagenesis to introduce basic residues (i.e. Arg; Lys) in the nucleic acid binding cleft of MMLV RT in order to increase its T/P binding affinity. Three stabilizing mutations (i.e. E286→R, E302→K, and L435→R) were identified. In this chapter, we studied the mechanism by which those mutations increase the thermal stability of the RT. The three single-mutants (E286R, E302K, and L435R), an RNase H-deficient MMLV RT (carrying the RNase H-inactivating mutation D524→A), a quadruple mutant (E286R/E302K/L435R/D524A, designated as MM4) and the wild-type enzyme (WT) were produced in *E. coli*. All RTs exhibited similar dissociation constants (K_d) for heteropolymeric DNA/DNA (2.9–6.5 nM) and RNA/DNA complexes (1.2–2.9 nM). Unlike the WT, mutant enzymes (E286R, E302K, L435R, D524A, and MM4) were devoid of RNase H activity, and were not able to degrade RNA in RNA/DNA complexes. These results suggest that the mutations, E286 →R, E302→K, and L435→R increase the thermostability of MMLV RT not by increasing its affinity for T/P but by abolishing its RNase H activity.

References

1. Roberts, J.D., Bebenek, K., Kunkel, T.A. (1988) The accuracy of reverse transcriptase from HIV-1. *Science* **242**, 1171-1173
2. Kimmel, A.R., Berger, S.L. (1987) Preparation of cDNA and the generation of cDNA libraries: overview. *Methods Enz.* **152**, 307-316
3. Kievits, T., van Gemen, B., van Strijp, D., Schukkink, P., Dircks, M., Adriaanse, H., Malek, L., Sooknanan, R., Lens, P. (1991) NASBA isothermal enzymatic in vitro nucleic acid amplification optimized for the diagnosis of HIV-1 infection. *J. Virol. Methods* **35**, 273-286
4. Ishiguro, T., Saitoh, J., Horie, R., Hayashi, T., Ishizuka, T., Tsuchiya, S., Yasukawa, K., Kido, T., Nakaguchi, Y., Nishibuchi, M., Ueda, K. (2003) Intercalation activating fluorescence DNA probe and its application to homogeneous quantification of a target sequence by isothermal sequence amplification in a closed vessel. *Anal. Biochem.* **314**, 77-86
5. Georgiadis, M.M., Jessen, S.M., Ogata, C.M., Telesnitsky, A., Goff, S.P., Hendrickson, W.A. (1995) Mechanistic implications from the structure of a catalytic fragment of Moloney murine leukemia virus reverse transcriptase. *Structure* **3**, 879-892
6. Das, D., Georgiadis, M.M. (2004) The crystal structure of the monomeric reverse transcriptase from Moloney murine leukemia virus. *Structure* **12**, 819-829
7. Lim, D., Gregorio, G.G., Bingman, C., Martinez-Hackert, E., Hendrickson, W.A., Goff, S.P. (2006) Crystal structure of the Moloney murine leukemia virus RNase H

domain. *J. Virol.* **80**, 8379-8389

8. Coté, M.L., Roth, M.J. (2008) Murine leukemia virus reverse transcriptase: structural comparison with HIV-1 reverse transcriptase. *Virus Res.* **134**, 186-202
9. Kohlstaedt, L.A., Wang, J., Friedman, J.M., Rice, P.A., Steitz, T.A. (1992) Crystal structure at 3.5 Å resolution of HIV-1 reverse transcriptase complexed with an inhibitor. *Science* **256**, 1783-1790
10. Bieth, E., Darlix, J.L. (1992) Complete nucleotide sequence of a highly infectious avian leukosis virus. *Nucleic Acids Res.* **20**, 367
11. Chien, A., Edgar, D.B., Trela, J.M. (1976) Deoxyribonucleic acid polymerase from the extreme thermophile *Thermus aquaticus*. *J. Bacteriol.* **127**, 1550-1557
12. Yasukawa, K., Nemoto, D., Inouye, K. (2008) Comparison of the thermal stabilities of reverse transcriptases from avian myeloblastosis virus and Moloney murine leukaemia virus. *J. Biochem*. **143**, 261-268
13. Berger, S.L., Wallace, D.M., Puskas, R.S., Eschenfeldt, W.H. (1983) Reverse transcriptase and its associated ribonuclease H: interplay of two enzyme activities controls the yield of single-stranded complementary deoxyribonucleic acid. *Biochemistry* **22**, 2365-2372
14. Gerard, G.F., Potter, R.J., Smith, M.D., Rosenthal, K., Dhariwal, G., Lee, J., Chatterjee, D.K. (2002) The role of template-primer in protection of reverse transcriptase from thermal inactivation. *Nucleic Acids Res.* **30**, 3118-3129
15. Masuda, N., Yasukawa, K., Isawa, Y., Horie, R., Saito, J., Ishiguro, T., Nakaguchi, Y., Nishibuchi, M., Hayashi, T. (2004) Rapid detection of *tdh* and *trh* mRNAs of *Vibrio parahaemolyticus* by the transcription-reverse transcription concerted (TRC) method. *J. Biosci. Bioeng.* **98**, 236-243

16. Yasukawa, K., Agata, N., Inouye, K. (2010) Detection of *cesA* mRNA from *Bacillus cereus* by RNA-specific amplification. *Enz. Microb. Technol*. **46**, 391-396
17. Das, D., Georgiadis, M.M. (2001) A directed approach to improving the solubility of Moloney murine leukemia virus reverse transcriptase. *Protein Sci.* **10**, 1936-1941
18. Bradford, M.M. (1976) A rapid and sensitive method for the quantitation of microgram quantities of protein utilizing the principle of protein-dye binding. *Anal. Biochem.* **72**, 248-254
19. Yasukawa, K., Mizuno, M., Inouye, K. (2009) Characterization of Moloney murine leukaemia virus/avian myeloblastosis virus chimeric reverse transcriptases. *J. Biochem.* **145**, 315-324
20. Laemmli, U.K. (1970) Cleavage of structural proteins during the assembly of the head of bacteriophage T4. *Nature* **227**, 680-685
21. Sakoda, M., Hiromi, K. (1976) Determination of the best-fit values of kinetic parameters of the Michaelis-Menten equation by the method of least squares with Taylor expansion. *J. Biochem.* **80**, 547-555
22. Liu, S., Goff, S.P., Gao, G. (2006) Gln^{84} of moloney murine leukemia virus reverse transcriptase regulates the incorporation rates of ribonucleotides and deoxyribonucleotides. *FEBS Lett.* **580**, 1497-1501
23. Arezi, B., Hogrefe, H. (2009) Novel mutations in Moloney murine leukemia virus reverse transcriptase increase thermostability through tighter binding to template-primer. *Nucleic Acids Res.* **37**, 473-481
24. Mizuno, M., Yasukawa, K., Inouye, K. (2010) Insight into the mechanism of the stabilization of Moloney murine leukaemia virus reverse transcriptase by eliminating RNase H activity. *Biosci. Biotechnol. Biochem.* **74**, 440-442

25. Konishi, A., Shinomura, M., Yasukawa, K. (2013) Enzymatic characterization of human immunodeficiency virus type 1 reverse transcriptase for use in cDNA synthesis. *Appl. Biochem. Biotechnol.*, **169**, 77-87
26. Baase, W.A., Liu, L., Tronrud, D.E., Matthews, B.W. (2010) Lessons from the lysozyme of phage T4. *Protein Sci.* **19**, 631-641
27. Chowdhury, K., Kaushik, N., Pandey, V.N., Modak, M.J. (1996) Elucidation of the role of Arg110 of murine leukemia virus reverse transcriptase in the catalytic mechanism: biochemical characterization of its mutant enzymes. *Biochemistry* **35**, 16610-16620
28. Yutani, K., Ogasahara, K., Tsujita, T., Sugino, Y. (1987) Dependence of conformational stability on hydrophobicity of the amino acid residue in a series of variant proteins substituted at a unique position of tryptophan synthase α subunit. *Proc. Natl. Acad. Sci. USA* **84**, 4441-4444
29. Shoichet, B.K., Baase, W.A., Kuroki, R., Matthews, B.W. (1995) A relationship between protein stability and protein function. *Proc. Natl. Acad. Sci. USA* **92**, 452-456
30. Arnórsdóttir, J., Helgadóttir, S., Thorbjarnardóttir, S.H., Eggertsson, G., Kristjánsson, M.M. (2007) Effect of selected Ser/Ala and Xaa/Pro mutations on the stability and catalytic property of a cold adapted subtilisin-like serine protienase. *Biochim. Biophys. Acta* **1774**, 749-755
31. Yasukawa, K., Inouye, K. (2007) Improving the activity and stability of thermolysin by site-directed mutagenesis. *Biochim. Biophys. Acta* **1774**, 1281-1288
32. Kusano, M., Yasukawa, K., Inouye, K. (2009) Insights into the catalytic roles of the polypeptide regions in the active site of thermolysin and generation of the

thermolysin variants with high activity and stability. *J. Biochem.* **145**, 103-113

33. Kusano, M., Yasukawa, K., Inouye, K. (2010) Effects of the mutational combinations on the activity and stability of thermolysin. *J. Biotechnol.* **147**, 7-16
34. Yasukawa, K., Konishi, A., Inouye, K. (2010) Effects of organic solvents on the reverse transcription reaction catalyzed by reverse transcriptases from avian myeloblastosis virus and Moloney murine leukemia virus. *Biosci. Biotechnol. Biochem.* **2010**, 1925-1930
35. Carninci, P., Nishiyama, Y., Westover, A., Itoh, M., Nagaoka, S., Sasaki, N., Okazaki, Y., Muramatsu, M., Hayashizaki, Y. (1998) Thermostabilization and thermoactivation of thermolabile enzymes by trehalose and its application for the synthesis of full length cDNA. *Proc. Natl. Acad. Sci. USA* **95**, 520-524
36. Arezi, B., McCarthy, M., Hogrefe, H. (2010) Mutant of Moloney murine leukemia virus reverse transcriptase exhibits higher resistance to common RT-qPCR inhibitors. *Anal. Biochem.* **400**, 301-303
37. Rariy, R.V., Klibanov, A.M. (1997) Correct protein folding in glycerol. *Proc. Natl. Acad. Sci. USA*, **94**, 13520-13523
38. Chen, Y., Xu, W., Sun, Q. (2009) A novel and simple method for high-level production of reverse transcriptase from Moloney murine leukemia virus (MMLV-RT) in *Escherichia coli*. *Biotechnol. Lett.* **31**, 1051-1057
39. Yasukawa, K., Mizuno, M., Konishi, A., Inouye, K. (2010) Increase in thermal stability of Moloney murine leukaemia virus reverse transcriptase by site-directed mutagenesis, *J. Biotechnol.* **150**, 299-306
40. Álvarez, M., Matamoros, T., Menéndez-Arias, L. (2009) Increased thermostability and fidelity of DNA synthesis of wild-type and mutant HIV-1 group O reverse

transcriptases. *J. Mol. Biol.* **392**, 872-884

41. Barrioluengo, V., Álvarez, M., Barbieri, D., Menéndez-Arias, L. (2011) Thermostable HIV-1 group O reverse transcriptase variants with the same fidelity as murine leukaemia virus reverse transcriptase. *Biochem. J.* **436**, 599-607
42. Schönbrunner, N.J., Fiss, E.H., Budker, O., Stoffel, S., Sigua, C.L., Gelfand, D.H., Myers, T.W. (2006) Chimeric thermostable DNA polymerases with reverse transcriptase and attenuated 3'-5' exonuclease activity. *Biochemistry* **45**, 12786-12795
43. Sano, S., Yamada, Y., Shinkawa, T., Kato, S., Okada, T., Higashibata, H., Fujiwara, S. (2012) Mutations to create thermostable reverse transcriptase with bacterial family A DNA polymerase from *Thermotoga petrophila* K4. *J. Biosci. Bioeng.* **113**, 315-321
44. Konishi, A., Nemoto, D., Yasukawa, K., Inouye, K. (2011) Comparison of the thermal stabilities of the αβ heterodimer and the α subunit of avian myeloblastosis virus reverse transcriptase. *Biosci. Biotechnol. Biochem.* **75**, 1618-1620
45. Gutiérrez-Rivas, M., Ibáñez, Á., Martínez, M.A., Domingo, E., Menéndez-Arias, L. (1999) Mutational anlaysis of Phe160 within the "palm" subdomain of human immunodeficiency virus type 1 reverse transcriptase. *J. Mol. Biol.* **290**, 615-625
46. Betancor, G., Puertas, M.C., Nevot, M., Garriga, C., Martínez, M.A., Martinez-Picado, J., Menéndez-Arias, L. (2010) Mechanisms involved in the selection of HIV-1 reverse transcriptase thumb subdomain polymorphisms associated with nucleoside analogue therapy failure. *Antimicrob. Agents Chemother.* **54**, 4799-4811
47. Beilhartz, G.L., Wendeler, M., Baichoo, N., Rausch, J., Le Grice, S., Götte, M.

(2009) HIV-1 reverse transcriptase can simultaneously engage its DNA/RNA substrate at both DNA polymerase and RNase H active sites: implications for RNase H inhibition. *J. Mol. Biol.* **388**, 462-474

48. Nowak, E., Potrzebowski, W., Konarev, P.V., Rausch, J.W., Bona, M.K., Svergun, D.I., Bujnicki, J.M., Le Grice, S.F.J., Nowotny, M. (2013) Structural analysis of monomeric retroviral reverse transcriptase in complex with an RNA/DNA hybrid. *Nucleic Acid Res.* **41**, 3874-3887
49. Zhou, D., Chung, S., Miller, M., Le Grice, S.F.J., Wlodawer, A. (2012) Crystal structures of the reverse transcriptase-associated ribonuclease H domain of xenotropic murine leukemia-virus related virus. *J. Struct. Biol.* **177**, 638-645
50. Telesnitsky, A., Goff, S.P. (1993) RNase H domain mutations affect the interaction between Moloney murine leukemia virus reverse transcriptase and its primer-template. *Proc. Natl. Acad. Sci. USA* **90**, 1276-1280
51. Barrioluengo, V., Wang, Y., Le Grice, S.F.J., Menéndez-Arias, L. (2012) Intrinsic DNA synthesis fidelity of xenotropic murine leukemia virus-related virus reverse transcriptase. *FEBS J.* **279**, 1433-1444
52. Kotewicz, M.L., D'Alessio, J.M., Driftmier, K.M., Blodgett, K.P., Gerard, G.F. (1985) Cloning and overexpression of Moloney murine leukemia virus reverse transcriptase in *Escherichia coli. Gene* **35**, 249-258
53. Konishi, A., Yasukawa, K., Inouye, K. (2012) Improving the thermal stability of avian myeloblastosis virus reverse transcriptase α-subunit by site-directed mutagenesis. *Biotechnol. Lett.* **34**, 1209–1215
54. Nishimura, K., Shinomura, M., Konishi, A., Yasukawa, K. (2013) Stabilization of human immunodeficiency virus type 1 reverse transcriptase by site-directed

mutagenesis. *Biotechnol. Lett.* **35**, 2165-2175

55. Goedken, E.R., Marqusee, S. (1999) Metal binding and activation of the ribonuclease H domain from Moloney murine leukemia virus. *Protein Eng.* **12**, 975-980

Acknowledgements

This study was carried out in the Laboratory of Enzyme Chemistry, Division of Fool Science and Biotechnology, Graduate School of Agriculture, Kyoto University, from 2009 to 2015.

I am deeply grateful to Dr. Kiyoshi Yasukawa, Professor of Kyoto University, for his invaluable guidance, kind support, and constant encouragement.

I wish to acknowledge the Dr. Kuniyo Inouye, Professor Emeritus of Kyoto University, for his tutelage with ardent interest in Enzyme Chemistry.

I am indebted to Dr. Teisuke Takita and Dr. Kenji Kojima, Assistant Professors of Kyoto University, for their incisive discussions.

I thank all other members of the Laboratory of Enzyme Chemistry.

I greatly appreciate the dedicated guidance and irreplaceable assistance from Dr. Luis Menéndez-Arias and Dr. Verónica Barrioluengo Fernández of Centro de Biología Molecular “Severo Ochoa”.

This study was supported by Grant-in-Aid for Japan Society for the Promotion of Science Fellows (No. 25-1955).

Finally, I give a special thanks to my family and friends for their assistance and encouragement.

March 2015

Atsushi Konishi

List of publications

Original papers

1. Yasukawa, K., Mizuno, M., Konishi, A., Inouye, K. (2010) Increase in thermal stability of Moloney murine leukaemia virus reverse transcriptase by site-directed mutagenesis. *J. Biotechnol.* **150**, 299-306
2. Konishi, A., Nemoto, D., Yasukawa, K., Inouye, K. (2011) Comparison of the thermal stabilities of the αβ heterodimer and the α subunit of avian myeloblastosis virus reverse transcriptase. *Biosci. Biotechnol. Biochem.* **75**, 1618-1620
3. Konishi, A., Yasukawa, K., Inouye, K. (2012) Improving the thermal stability of avian myeloblastosis virus reverse transcriptase α subunit by site-directed mutagenesis. *Biotechnol. Lett.* **34**, 1209-1215
4. Konishi, A., Ma, X., Yasukawa, K. (2014) Stabilization of Moloney murine leukemia virus reverse transcriptase by site-directed mutagenesis of the surface residue Val433. *Biosci. Biotechnol. Biochem.* **78**, 75-78
5. Konishi, A., Hisayoshi, T., Yokokawa, K., Barrioluengo, V., Menéndez-Arias, L., Yasukawa, K. (2014) Amino acid substitutions away from the RNase H catalytic site increase the thermal stability of Moloney murine leukemia virus reverse transcriptase through RNase H inactivation. *Biochem. Biophys. Res. Commun.* **454**, 269-274

Related papers

1. Yasukawa, K., Konishi, A., Inouye, K. (2010) Effects of organic solvents on the reverse transcription reaction catalyzed by reverse transcriptases from avian myeloblastosis virus and Moloney murine leukemia virus. *Biosci. Biotechnol. Biochem.* **74**, 1925-1930
2. Yasukawa, K., Konishi, A., Shinomura, M., Nagaoka, E., Fujiwara, S. (2012) Kinetic analysis of reverse transcriptase activity of bacterial family A DNA polymerases. *Biochem. Biophys. Res. Commun.* **427**, 654-658
3. Konishi, A., Shinomura, M., Yasukawa, K. (2013) Enzymatic characterization of human immunodeficiency virus type 1 reverse transcriptase for use in cDNA synthesis. *Appl. Biochem. Biotechnol.* **169**, 77-87, 2013
4. Nishimura, K., Shinomura, M., Konishi, A., Yasukawa, K. (2013) Stabilization of human immunodeficiency virus type 1 reverse transcriptase by site-directed mutagenesis. *Biotechnol. Lett.* **35**, 2165-2175
5. Hisayoshi, T., Shinomura, M., Konishi, A., Tanaka, J., Shimoda, H., Hata, K., Takahashi, S., Yasukawa, K. (2014) Inhibition of HIV-1 reverse transcriptase activity by *Brasenia schreberi* (Junsai) components. *J. Biol. Macromol.* **14**, 59-65